Ro-Vibrational levels and (e-f) splitting of acetylene molecule calculated from new potential energy surfaces

Andrei Nikitin, Alexander Protasevich, Alena Rodina, Michael M. Rey, Attila Tajti, Vladimir Tyuterev

Ro-Vibrational levels and (e-f) splitting of acetylene molecule calculated from new potential energy surfaces

Andrei V. Nikitin[1], Alexander E. Protasevich[1], Alena A. Rodina[1], Michael Rey[2], Attila Tajti [3], and Vladimir G. Tyuterev[2,4]

[1.] *V.E. Zuev Institute of Atmospheric Optics, Russian Academy of Sciences, 1, Akademichesky Avenue, 634055 Tomsk, Russian Federation*
[2.] *Groupe de Spectrométrie Moléculaire et Atmosphérique, UMR CNRS 6089, Université de Reims, U.F.R. Sciences, B.P. 1039, 51687 Reims Cedex 2, France*
[3.] *ELTE Eötvös Loránd University, Institute of Chemistry, Laboratory of Theoretical Chemistry, P. O. Box 32, H-1518, Budapest 112, Hungary*
[4] *QUAMER, Tomsk State University, 36 Lenin Avenue, 634050 Tomsk, Russian Federation*

Number of Pages: 32
Number of Figures: 11
Number of Tables: 7
Number supplemental files: 1

Running Head: Vibration energy levels of acetylene

Keywords: acetylene**, potential energy surface, vibrational energy levels, kinetic energy operator**

Correspondence should be addressed to:
Andrei V. Nikitin,
*Laboratory of Theoretical Spectroscopy, V.E. Zuev Institute of Atmospheric Optics, SB RAS, 1, Academician Zuev square, 634021, Tomsk, Russia
E-mail: avn@iao.ru
Phone : +73822 – 491111 (ext. 1208)

Abstract

Ro-vibrational energy levels of C_2H_2 are reported using variational nuclear motion calculations from new ab initio and empirically optimized full six-dimensional ab initio potential energy surfaces in the ground electronic state of the acetylene molecule. Ab initio calculations are based on extended electronic structure coupled-cluster calculations for dynamic electron correlations. The calculations account for the triple, quadruple and pentuple excitations as well as relativistic and diagonal Born-Oppenheimer corrections. Variational nuclear motion calculations were performed using the exact kinetic energy operator in orthogonal coordinates. The convergence of energy levels calculations versus the size of the vibrational basis set functions was verified. Our best ab initio potential energy surface that includes the above mentioned contributions provides the RMS (obs.-calc.) errors of 0.95 cm^{-1} for five fundamental energy levels. The largest contribution to the RMS error is caused primarily by a significant deviation of the ν4 fundamental frequency. Experimental values of 120 vibrational band origins were used to empirically adjust few lower-order parameters of the potential energy surface. The average error drops down to 0.45 cm^{-1} or 0.25 cm^{-1} for empirically optimized potential energy function with two or seven adjusted parameters corresponding to quadratic force field terms and one third order term. The splitting of (e – f) rovibrational doublets and their J dependence were calculated with high accuracy due to the full account of Coriolis interactions. Computed (e – f) splittings allow us to check the correctness of the assignment of empirical energy levels. The estimation of the accuracy for the calculated vibrational levels in an extended range up to 9500 cm^{-1} shows that the set of ab initio vibrational levels can be used for future assignmens of empirically unknown ro-vibrational energy levels. The comparison of the calculated and experimental ro-vibrational energy levels of the C_2D_2 and $^{13}C_2H_2$ isotopologues is also reported.

Introduction

Calculation of energy levels for acetylene molecule from the force field parameters or from the potential energy surface (PES) with application to spectroscopy analyses was the subject of many studies during last decades [**1**] [**2**] [**3**] [**4**] [**5**] [**6**] [**7**] [**8**] [**9**] [**10**] [**11**] [**12**] [**13**] [**14**] [**15**] [**16**] [**17**]. Acetylene is one of the most studied species among four-atomic linear molecules [**18**] [**19**] [**20**] [**21**] [**22**] [**23**]. A large set of empirically determined energy levels has been obtained in [**24**] [**25**] [**26**] [**27**] [**28**] [**29**] [**23**] due to the importance of acetylene

absorption/emission spectra for various applications [**30**] [**31**] [**17**]. The PES appears to be flat with respect to the torsion angle near the linear equilibrium geometry if one of the CCH angles is close to π. For this reason, the vibrational wave functions are delocalized toward the torsion degree of freedom for the corresponding set of geometrical configurations. In this context the calculation of energy levels faces some problems similar to those of nonrigid molecules. For linear A_2B_2 molecules, there remain 9 vibrational-rotational degrees of freedom after excluding the translational motion. It is well-known that the separation between vibrational and rotational degrees of freedom is different in the case of linear and non-linear molecules [**32**]. This requires a special care for the basis set construction in variational calculations [**33**], particularly in case of flat PES cuts in some vibrational motions as we have for the acetylene molecule.

The point group of the equilibrium geometrical configuration of an A_2B_2 linear molecule is $D_{\infty h}$ that possesses non-degenerate $\Sigma^{\pm}_{u/g}$ and an infinite number of doubly degenerate irreducible representations $\Pi_{u/g}$, $\Delta_{u/g}$, … which are often used to label energy levels. However, when the vibrational-rotational motions are excited, the molecule is no longer linear [**34**] [**35**], and it is more appropriate to consider molecular symmetry groups defined as $D_{\infty h}(M)$ [**36**], [**37**], accounting for permutation-inversion operations of identical nuclei. This latter one is isomorphic to the Klein abelian group [**38**] possessing only 4 elements and 4 one-dimensional irreducible representations. Thus rovibrational wave functions for each J value are partitioned into four isolated blocks distinguished by the parity under inversion p and the parity under permutation σ of identical nuclei. The states with even value of $J + p$ are labeled by e, whereas the states with the odd value of by f [**39**]. Even $\sigma + p$ values correspond to g states and odd values to u states. The Hamiltonian eigenvalues in various blocks are, in general, different. There appear *e/f* doublets in rovibrational energy levels spitted by the Coriolis interactions. In this work we show that the ($e - f$) splitting for these doublets can be very accurately predicted from ab initio PES for various J values. Note that in ref. [**40**] an artificial, formally infinite molecular symmetry group $D_{\infty h}(AEM)$ has been introduced for linear molecules, but wave functions were finally classified according to one-dimensional representations.

The spectroscopic data of acetylene including highly excited states are important due to a wide range of applications: it is used as a fuel and in industrial applications linked to the high temperature of the flame. The acetylene is involved in various reactions as a chemical building block and serves for carbon dating of organic materials. It was found in atmospheres of giant planets and exoplanets. The accurate knowledge of rovibrational transitions is important for the interpretation of near-infrared spectra in the ground-based and satellite observatories [**41**] [**42**].

The development of efficient methods for variational nuclear motion calculations based on ab initio potential energy surfaces (PES) and of dipole moment surfaces (DMS) has permitted significant progress in predictions of vibrational-rotational bands. This was, for example, the case with the spectroscopy of water [**43**] [**44**] [**45**] [**46**], carbon dioxide [**47**] [**48**] [**49**], hydrogen sulfide [**50**] [**51**], sulfur dioxide [**52**], and ozone [**53**] [**54**] [**55**]. In the latter case, ab initio predictions were used for precise quantification [**56**] of band intensities, for understanding the PES properties in the transition state range towards the dissociation threshold [**57**] [**55**], the interactions between potential wells [**58**], and modeling of the isotopic exchange reactions [**59**].

Recently, theoretical calculations of rotationally resolved spectra have helped extending assignments and modeling of high-resolution spectra for 4,5, and 6 atomic molecules [**60**] [**61**] [**62**] [**63**] [**64**], including hot bands. Many ab initio PESs have been subsequently refined by a fit to experimental data to achieve better accuracy in line positions. Theoretical line lists for ammonia [**65**] [**49**] [**66**] and phosphine [**67**] [**68**] [**69**] are successful examples of this trend for four-atomic species. New PESs and DMSs have been recently reported for five-atomic [**70**] [**71**], six-atomic [**72**] [**73**], [**74**] and seven-atomic [**75**] molecules.

In the present work, we report theoretical vibrational levels of acetylene computed from a new accurate ab initio PES using the algorithms similar to the one recently applied for the methane [**76**] and formaldehyde molecules [**77**] [**78**] and compare our results with other recent calculations [**77**] [**79**] and with experimental data. A very large set of observations for acetylene makes this molecule an interesting benchmark object for high-level quantum-chemical calculations. For many-electron molecules, the "spectroscopic accuracy" in ab initio vibrational levels of about 0.1 cm^{-1} (at least in the low and medium energy ranges) was achieved in few works as reported in refs. [**46**], [**80**] for the water molecule, and in ref. [**76**] for methane. Both of these molecules contain 10 electrons, whereas the acetylene molecule has 14 electrons. Two recent studies [**77**] [**78**] reported quite accurate theoretical calculations for formaldehyde (16 electrons), that gave a hope to achieve similar results for acetylene as well.

In contrast to formaldehyde, acetylene is an experimentally much better studied molecule, but due to symmetry properties the origins ($J=0$ levels) for many acetylene bands cannot be observed directly. They are usually implicitly deduced from experimental spectra using effective rotational constants. For this reason, a reliable comparison with observation cannot be limited to purely vibrational levels and has to include $J > 0$ series. The corresponding calculations reported in this paper can be considered as an additional source of information that could be useful for the extended assignment and modeling of high-resolution experimental spectra of acetylene and its isotopologues.

The paper is structured as follows. The choice of the coordinates and the analytical representations for the PES and their comparison in terms of the flexibility of the fit of ab initio electronic energy points on the geometrical grid is discussed in Section 1. Exact kinetic energy operator (KEO), ro-vibrational calculations, and the basis set convergence for the nuclear motion are discussed in Section 2. Section 3 is devoted to the study of the dependence of the theoretical vibrational levels on the electronic basis set. The impact of relativistic corrections, diagonal Born-Oppenheimer corrections (DBOC), and of high-order electron correlation including connected triple and quadruple excitations in the coupled-cluster method is also considered. A detailed comparison with available experimental data in Sections 3 and 5 shows that the resulting full-dimensional ab initio PES provides currently the most accurate theoretical band origins and low-J rotational levels for acetylene. The high-precision calculations of the (e-f) splitting of rovibrational levels due to Coriolis interactions and their J-dependence are discussed in Section 4. Two versions of an empirically optimized PES obtained with a fine tuning of two and seven PES parameters and the corresponding predicted vibrational levels are also reported.

1. Coordinates and analytical PES representation

For calculations of the vibrational-rotational energy levels of the acetylene molecule we used the kinetic energy operator (KEO) in the orthogonal coordinates [**81**] [**8**] [**82**] [**83**] written in the form originally presented in ref [**84**].

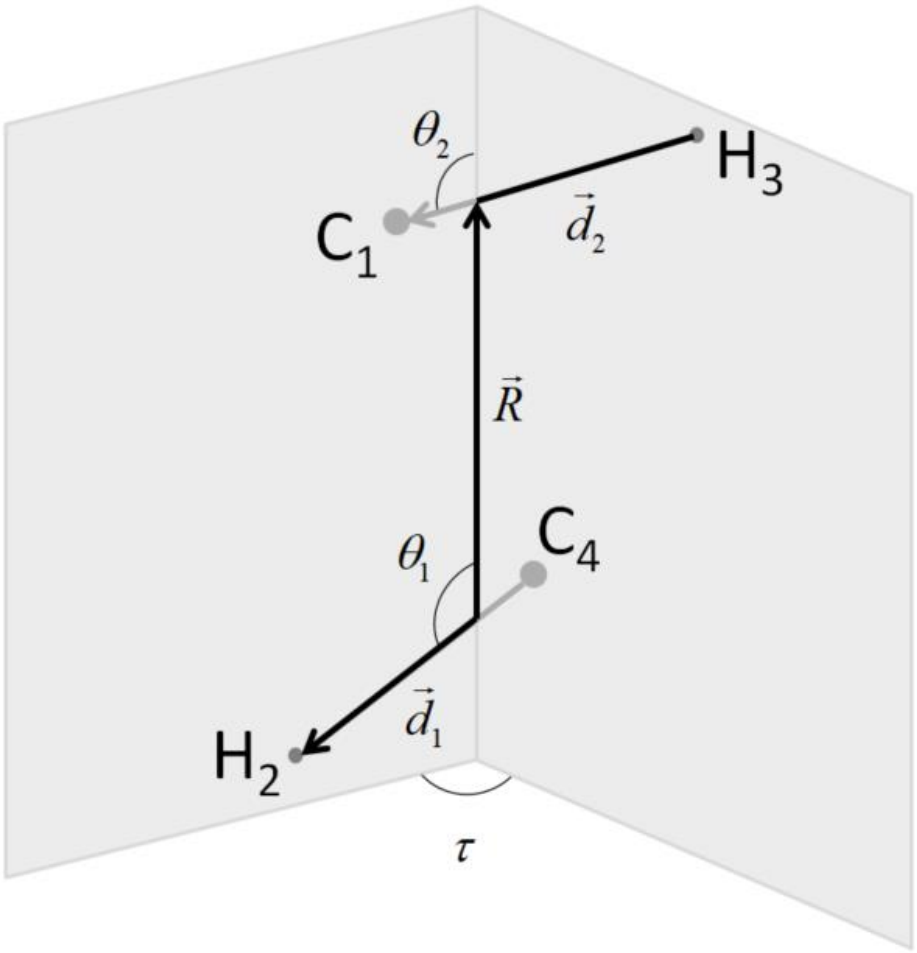

Figure 1. Vectors of Jacobi coordinates for the acetylene molecule.

The positions of atoms in the molecular fixed coordinates (MFC) are related to their positions in the laboratory system R_i as follows: (see Figure 1).

$$\boldsymbol{R} = \frac{m_1\mathbf{R_1}+m_3\mathbf{R_3}}{m_1+m_3} - \frac{m_2\mathbf{R_2}+m_4\mathbf{R_4}}{m_2+m_4},\ \boldsymbol{d_1} = \mathbf{R_2} - \mathbf{R_4},\ \boldsymbol{d_2} = \mathbf{R_1} - \mathbf{R_3}, \quad (1)$$

with m_1 , m_4 being the nuclear mass of carbon and m_2 , m_3 those of hydrogen. The PES is expressed as a power series of elementary functions in the symmetrized coordinates involving Morse-type functions for "radial" and a sine function of angular variables:

$$V(d_1, R, d_2, \theta_1, \theta_2, \tau) = \sum_{ijklmn} f_{ijklmn} S_1^i S_2^j S_3^k S_4^l S_5^m S_6^n \text{ , where} \quad (2)$$

$$S_1 = \left(y(d_1) + y(d_2)\right)/\sqrt{2},\quad S_2 = y(R),\quad S_5 = \left(y(d_1) - y(d_2)\right)/\sqrt{2}, \quad (3)$$

$$S_3 = \left(f(\theta_1) + f(\theta_2)\right)/\sqrt{2},\quad S_6 = \left(f(\theta_1) - f(\theta_2)\right)/\sqrt{2},\quad S_4 = f\left(\tau\right). \quad (4)$$

A Morse-type function $y(d) = 1 - \exp(-a(d - d_e))$ with the parameter *a=1.9* is used as the radial function, and $f(\theta) = \sin((\pi - \theta)/2)$ is used as the angular function. The torsion angle τ is the angle between the $d_1 \times R$ and $d_2 \times R$ planes. It is obvious that the symmetry group used for constructing the PES contains only two generating elements: the permutation of coordinates (12) of identical nuclei and the operation of reflection in the plane that inverts the sign of τ. This group is isomorphic to the Abelian C_{2v} point group, or the Klein group [**38**]. Therefore, we use almost the same analytical representation for the PES shape as for the H_2CO molecule [**78**]. The only exception concerns some terms in Eq.(2) in which there is no dependence on the angle for k=0 and n=0. These terms also cannot depend on the angle τ. Therefore, the parameters corresponding to k=0 and n=0 and l>0 were not included in the expression (2). The $\cos(\tau), \cos(\tau/2)$ functions were tested as the torsion function $S_4 = f(\tau)$. The first function transforms as the A_1 irreducible representation while the second function transforms as B_1. We also tested other forms of the function $f(\theta)$, but finally the form $\sin((\pi - \theta)/2)$ was preferred.

In the present study, we applied the same tensor techniques for an optimal sampling of the grid of nuclear configurations as described in our previous works for non-abelian symmetry groups [**85**] [**86**]. This permitted accounting for the full symmetry of the molecule in order to reduce the number of geometrical nuclear configurations for the ab initio calculation of electronic energies. To build the corresponding grid of geometries, we used one-dimensional sections of the PES. Though the radial one-dimensional sections are similar to the corresponding sections of formaldehyde, the angular sections differ considerably. Figure 2 shows two angular one-dimensional sections *S3*, *S6* and four torsional sections for $\pi - \theta_1 = \pi - \theta_2 = 10,\ 20, 40, 60$ degrees. It is evident that the dependence on the torsion angle is weak at small energies.

To describe the PES up to the 12-th order of the expansion (2) in general (but limited to the 6-th order for CH radial coordinates), a grid of geometries was built. The corresponding initial reference grid (G(R)) contained 4876 points. Additionally, a grid of 7171 geometries (with a step of 30 degrees within the range of 0 - 180 degrees) was built to refine the description of the torsion dependence at the bottom of the potential well at energies up to 5000 cm^{-1}. Thus, the largest grid included 12047 geometries.

The set of the grid points was chosen in a way which ensures that a maximum number of parameters of our analytical PES representation would be well-defined in the least-squares fits to the calculated ab initio electronic energies. The PES parameters responsible for the coupling

among various vibrational modes were systematically included. This relatively dense grid provides a possibility for testing various high-order PES expansions in elementary functions of the symmetrized coordinates. The initial grid of points was arranged in a way that their energy cut-off would correspond to the extent of the studied infrared bands. For this grid, the initial calculations were carried out with the coupled-cluster CCSD(T) method using the quintuple-zeta cc-pACV5Z [**87**] basis set (referred to as ACV5Z sets in abbreviated notation), and the MOLPRO quantum chemistry program package [**88**] [**89**].

To validate various representations of the PES using the least-squares technique, an extended grid of geometries was used. As in the case of formaldehyde, the grid was augmented by adding supplementary sets of points corresponding to 180-τ values (for $\tau \neq 180$) in the initial grid.

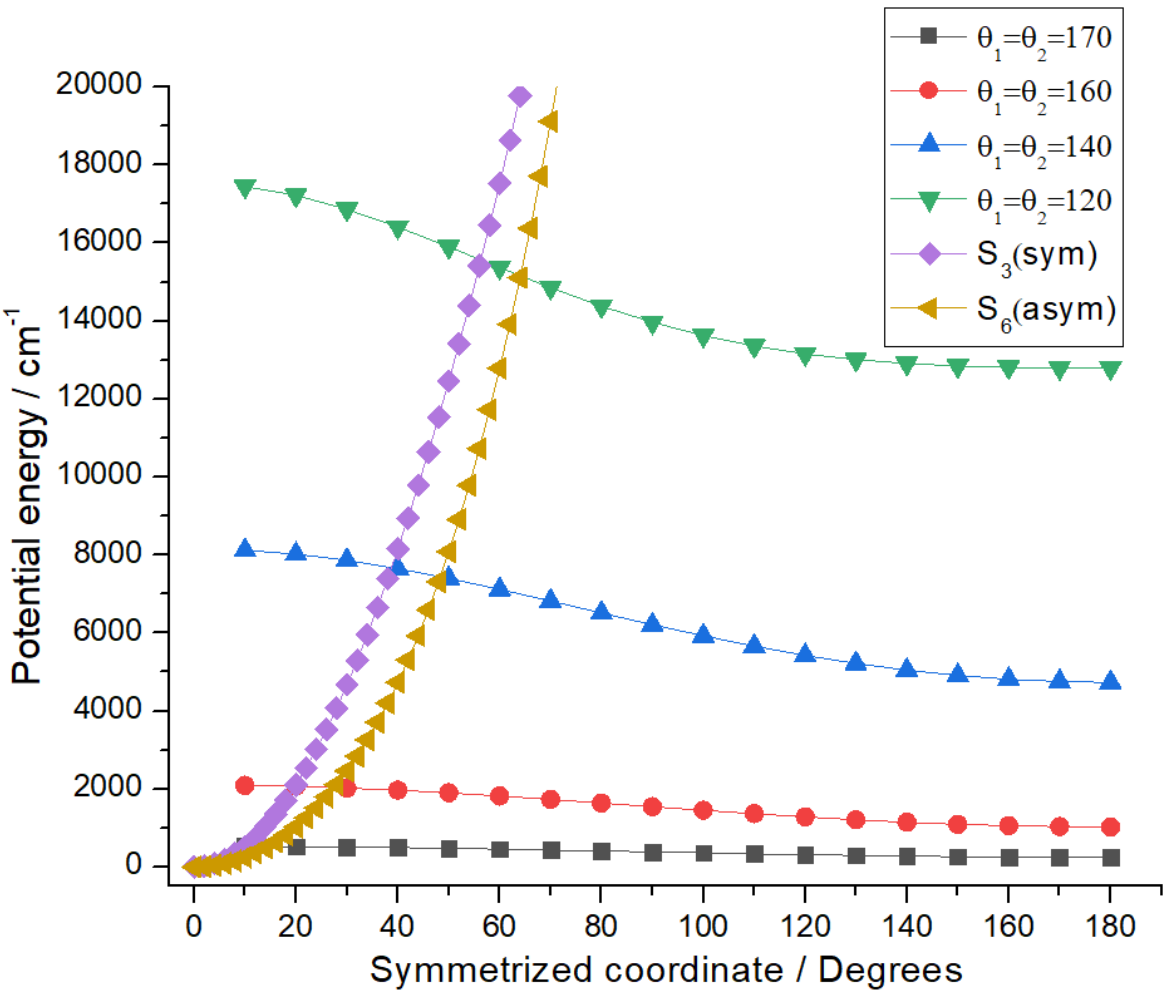

Figure 2. One-dimensional PES sections for angular symmetrized coordinates S_3, S_6, and torsion sections for $\pi - \theta_1 = \pi - \theta_2 = 10, 20, 40, 60$ degrees.

To compare the efficiency of the analytical form (2) in various coordinate sets, the benchmark PES calculations were carried out using a least-squares fit to the ACV5Z grid values, without corrections discussed in the following sections. Even though the ACV5Z basis set does not provide the best quantitative accuracy, we believe that it is preferable to use all PESs at the same theoretical level, without corrections for a reliable comparison of the general qualitative shape of the surfaces. A*b initio* potential energies were fitted using the analytical symmetry adapted representation (2)-(4), and the weight function employed by Schwenke and Partridge in ref [**83**]:

$$w(E) = \frac{\tanh(-0.0005\,(E - E_1) + 1.00200200\ \ 2)}{2.00200200\ \ 2}. \qquad (5)$$

The weight function defined in equation (5) decreases with the energy E (expressed in cm^{-1}) in order to de-emphasize the contribution of large grid displacements for vibrational energies beyond E_1=15000 cm^{-1} to the PES fit. The least-squares fit of the PES in various sets of coordinates leads to similar results. The row III of Table 1 shows the number of parameters which were statistically well determined by fitting of the PES to ab initio electronic energies, versus the total number of parameters of the corresponding order of the expansion. The PES III contains all sixth-order terms augmented by 8^{th} order angular terms, but the overall fit is not better than for the PES I. Although the fit of the PES II is slightly better than that of PES I, the energy levels up to 7000 cm^{-1} obtained from these two PESs are close, but the calculation of energy levels with the PES I is considerably faster.

Table 1. RMS and standard deviations of the PES fits in various coordinate sets.

Set	I	II	III
Order of expansion	6	7	6 plus
Torsion function	$\underline{\cos(\tau)}$	$\underline{\cos(\tau)}$	$\underline{\cos(\tau/2)}$
#Parameters/Initial # Param	304/422	408/771	320/493
RMS (STD)	0.96 (0.97)	0.57(0.59)	0.99(0.79)

Table 2 gives the equilibrium geometry parameters. It can be seen that the calculation using the CV6Z basis set gives smaller equilibrium distances in comparison to CV5Z. Figure 6 shows that ACV6Z gives a shorter distance in comparison to ACV5Z. To expand the PES, we use the CCSD(T) / ACV5Z value of the equilibrium geometry as described in our previous works [**76**], [**78**]. For CCSD(T) / ACV5Z, the r_e(CC) and r_e(CH), distances in the equilibrium geometry are slightly larger than the values optimized using standard quantum chemical procedures. Note that due to the presence of linear terms in the expansion of the potential, the vibrational-rotational levels in our calculations practically do not depend on the reference geometry point with respect to which the PES is expanded in a Taylor series.

Table 2. Equilibrium geometry of the C_2H_2 molecule, as optimized at various levels of ab initio theory

Coordinates	CCSD(T)/ pwCVQZ	CCSD(T)/ ACVQZ	CCSD(T) / ACV5Z	CCSD(T)/ ACV5Z-DK**	CCSD(T) / CV5Z	CCSD(T) / CV6Z
r_e(CC) / Å	1.20341713	1.20403710	1.20305941	1.20278890	1.20289953	1.20262992
r_e(CH) / Å	1.06210688	1.06236424	1.06185072	1.06168717	1.06173152	1.06166908

** Accounting for Douglas-Kroll-Hess relativistic corrections denoted DK in what follows.

2. Rovibrational calculations

The rotational-vibrational wave function is constructed in the form

$$\left|J,M,l_1,m_1,l_2,m_2\right\rangle \equiv \sqrt{2\pi}Y_{l_1m_1}\left(\theta_1,\varphi_1\right)Y_{l_2m_2}\left(\theta_2,\varphi_2\right)\left(\left|J,m_1+m_2,M\right\rangle\right|_{\gamma=0}\Big), \tag{6}$$

where $Y_{lm}\left(\theta,\varphi\right)$ are spherical functions [**90**], and

$\left|J,K,M\right\rangle \equiv \sqrt{\frac{2J+1}{8\pi^2}}\exp\left(iM\alpha\right)d^J_{MK}\left(\beta\right)\exp\left(iK\gamma\right)$ – is a symmetric top fuction [**91**], depending on the Euler angles α, β, γ, which determine the orientation of the molecule frame system (MFS) with respect to the laboratory frame (LF) , and $\varphi_1=\gamma$, $\varphi_2=\gamma+\tau+\pi$ (instead of $\varphi_2=\gamma+\tau$ in Ref. [**84**]). Note that in (6), the sum m_1+m_2 plays the role of *K* (the projection onto the Z axis in the MFS) in the $\left|J,K,M\right\rangle$ function. Therefore, in this work, we use the notation : $K=m_1+m_2$. The kinetic energy operator from Ref [**84**] was used for the calculation of energy levels.

$$\hat{T}^{\text{ortho}} = -\frac{\hbar^2}{2M\mu_{d_1}}\left(\frac{\partial^2}{\partial d_1^2}+\frac{2}{d_1}\frac{\partial}{\partial d_1}\right)-\frac{\hbar^2}{2M\mu_{d_2}}\left(\frac{\partial^2}{\partial d_2^2}+\frac{2}{d_2}\frac{\partial}{\partial d_2}\right)-\frac{\hbar^2}{2M\mu_R}\left(\frac{\partial^2}{\partial R^2}+\frac{2}{R}\frac{\partial}{\partial R}\right)+$$
$$+\frac{1}{2M}\left(\frac{1}{\mu_{d_1}d_1^2}+\frac{1}{\mu_R R^2}\right)\hat{l}_1^2+\frac{1}{2M}\left(\frac{1}{\mu_{d_2}d_2^2}+\frac{1}{\mu_R R^2}\right)\hat{l}_2^2+ \tag{7}$$
$$+\frac{1}{2M\mu_R R^2}\left(\hat{J}^2+2\hat{l}_{1z}\hat{l}_{2z}-2\hat{J}_z^2+\left(\hat{l}_2^+\hat{l}_1^-+\hat{l}_2^-\hat{l}_1^+\right)-\left(\hat{l}_2^-+\hat{l}_1^-\right)\hat{\tilde{J}}^- -\left(\hat{l}_2^++\hat{l}_1^+\right)\hat{\tilde{J}}^+\right),$$

where M – is the total nuclear mass of the molecule ; μ_{d_1} , μ_{d_2} and μ_R are the dimensionless masses: $\mu_{d_1}=2m_Cm_H/M^2$, $\mu_{d_2}=2m_Cm_H/M^2$ and $\mu_R=1/4$, (where m_C and m_H are the masses of the nuclei C and H, respectively), d_1, d_2 and R are the lengths of the internuclear

vectors connecting the nuclei C_4 and H_2, the nuclei C_1 and H_3, and the centers of mass of the CH nuclear groups, respectively (see Figure 1), and the operators *l, J* in (7) are:

$$\hat{l}_{jz} = -i\hbar\frac{\partial}{\partial\varphi_j}, \qquad \hat{l}_j^{\pm} = -\exp\left(\pm i\varphi_j\right)\left(\mp\hbar\frac{\partial}{\partial\theta_j} + \mathrm{ctg}\theta_j\,\hat{l}_{jz}\right), \qquad (j=1,2)$$

$$\hat{J}_z = \hat{l}_{1z} + \hat{l}_{2z}, \quad \hat{\tilde{J}}^{\pm} \equiv \exp\left(\mp i\varphi_1\right)\hat{J}^{\pm} = \mathrm{ctg}\beta\hat{J}_z \mp \hbar\frac{\partial}{\partial\beta} + i\hbar\frac{1}{\sin\beta}\frac{\partial}{\partial\alpha}$$

Ref [**84**] introduced a basis adapted for parity with respect to space inversion:

$$\left|J,M,p,l_1,m_1,l_2,m_2\right\rangle \equiv \left(\left|J,M,l_1,m_1,l_2,m_2\right\rangle + (-1)^{J+p}\left|J,M,l_1,-m_1,l_2,-m_2\right\rangle\right)/\sqrt{2\left(1+\delta_{m_1 0}\delta_{m_2 0}\right)}, \quad (8)$$

where $p=\{0,1\}$, $|m_1| \le l_1 \le L_{\max}$, $|m_2| \le l_2 \le L_{\max}$, $0 \le m_1 + m_2 \le J$

The basis of Eq.(8) can be adapted to the symmetry that corresponds to the permutation of identical atoms. This basis is described in Section 4 below. On the other hand, the basis (8) can be adapted to the complete symmetry in a simpler way by contracting the set of angular functions. The contraction of the angular basis (8) is necessary because of its large dimension. For example, for *L_{max}=28*, and p=0, the number of functions (8) with values of $m_1 + m_2$ equal to 0, 5, 10, 15, 20 is 8555, 15604, 13864, 104200, and 122639, respectively. Due to the rapid increase of the energy with increasing $m_1 + m_2$, the angular basis vectors with $m_1 + m_2 > 10$ are far beyond a natural cut-off for the considered range of applications. In addition, spectral transitions to energy levels for which the vectors $m_1 + m_2 > 3$, produce contributions to very weak ines inaccessible for experimental registration. When contracting, the eigenfunctions of the operator

$$\hat{T}^{\text{ortho angular}} = \frac{1}{2M}\left(\frac{1}{\mu_{d_1}d_1^2} + \frac{1}{\mu_R R^2}\right)\hat{l}_1^2 + \frac{1}{2M}\left(\frac{1}{\mu_{d_2}d_2^2} + \frac{1}{\mu_R R^2}\right)\hat{l}_2^2 \qquad (9)$$

for fixed $m_1 + m_2$ values are used as an angular basis set. When solving the ro-vibrational problem with the KEO of Eq. (9) at certain value of *J*, the eigenfunctions for $K = m_1 + m_2 \le J$ in the low energy range are chosen in the following form:

$$F_n^{K,p} = \sum_{l_1,l_2,m_1,m_2,m_1+m_2=K} c_{l_1,l_2,m_1,m_2}^{K,p}\left|K,0,p,l_1,m_1,l_2,m_2\right\rangle. \qquad (10)$$

The eigenfunctions $F_n^{K,p}$ defined by Eq.(10) are either symmetric or antisymmetric versus the permutation of the pairs of indices $(l_1,m_1) \leftrightarrow (l_2,m_2)$ with a high degree of accuracy. Below, we

denote such a permutation operator as $\hat{\sigma}$ with eigenvalues σ, which will be added as upper case indices to the functions $F_n^{K,p,\sigma}$ to specifiy their parity.

To select an optimal basis set, an analysis of the convergence of vibrational-rotational energy levels was made. The dependence of the quantized angular energies on the parameter L_{max} is shown in Figure 3. It is evident that up to 8000 cm^{-1} the convergence is no worse than 10^{-3} cm^{-1} and $L_{max}=28$ is quite sufficient for convergence. The convergence of energy levels at $J=20$ depending on the number of angle functions is shown in Figure 3. Figure 4 shows the convergence of the angular energy levels at $J=20$ depending on the number of angle functions. It can be seen that for $J=20$ a sufficiently high number of angular functions is required. At the same time, as a rule, the transition intensities for highly excited angular functions are low. Therefore, 1200 or 1800 angular functions are quite sufficient for a calculation of spectra at room temperature.

Figure 5 shows the convergence of vibrational energy levels depending on the number of radial functions. Below 4500 cm^{-1}, the influence of the PES type on the energy levels is not significant: the differences in the level values do not exceed 0.1 cm^{-1}.

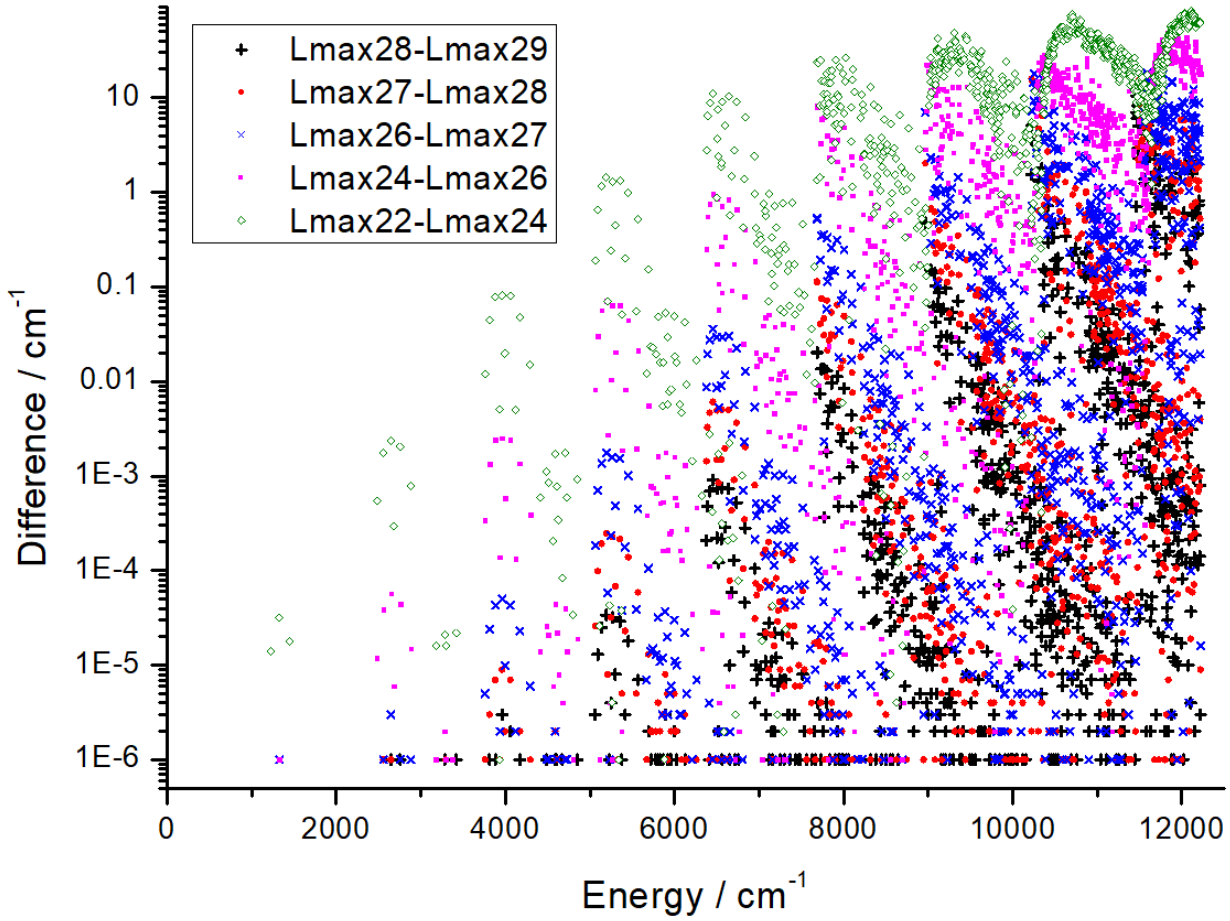

Figure 3. The basis set convergence of angular functions versus the parameter L_{max}. The difference between angular energy levels calculated for nearby values of L_{max} is depicted with different color codes. The descrepancies between two largest basis sets shown with black crosses indicate the convergence of the order of 0.1-0.01 cm^{-1} in the vibrational energy range up to about 8000-10000 cm^{-1}.

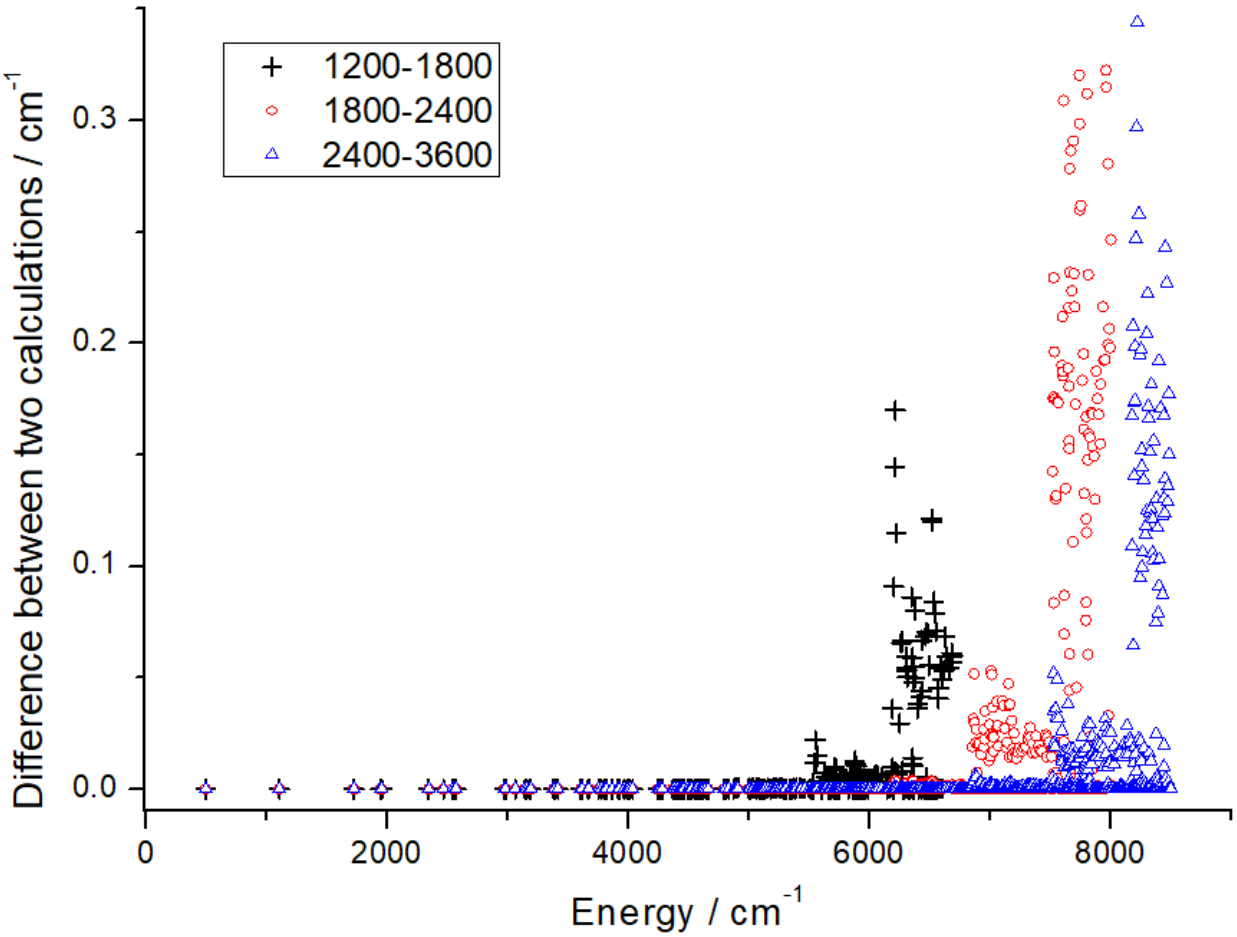

Figure 4. Convergence of angular energy levels E_a at $J=20$, $p=0, \sigma=0$. The descrepancies ΔEa between two calculations using increasing numbers N_a of angular basis functions are depicted :

Ea (Na=1800) - (Na=1200) up to 6800 cm^{-1} in black crosses; Ea (Na=2400) - (Na=1800) up to 8000 cm^{-1} in red circles; Ea (Na=3600) - (Na=2400) up to 8700 cm^{-1} in red circles. The values of $L_{max}=28$ are held fixed for all calculations.

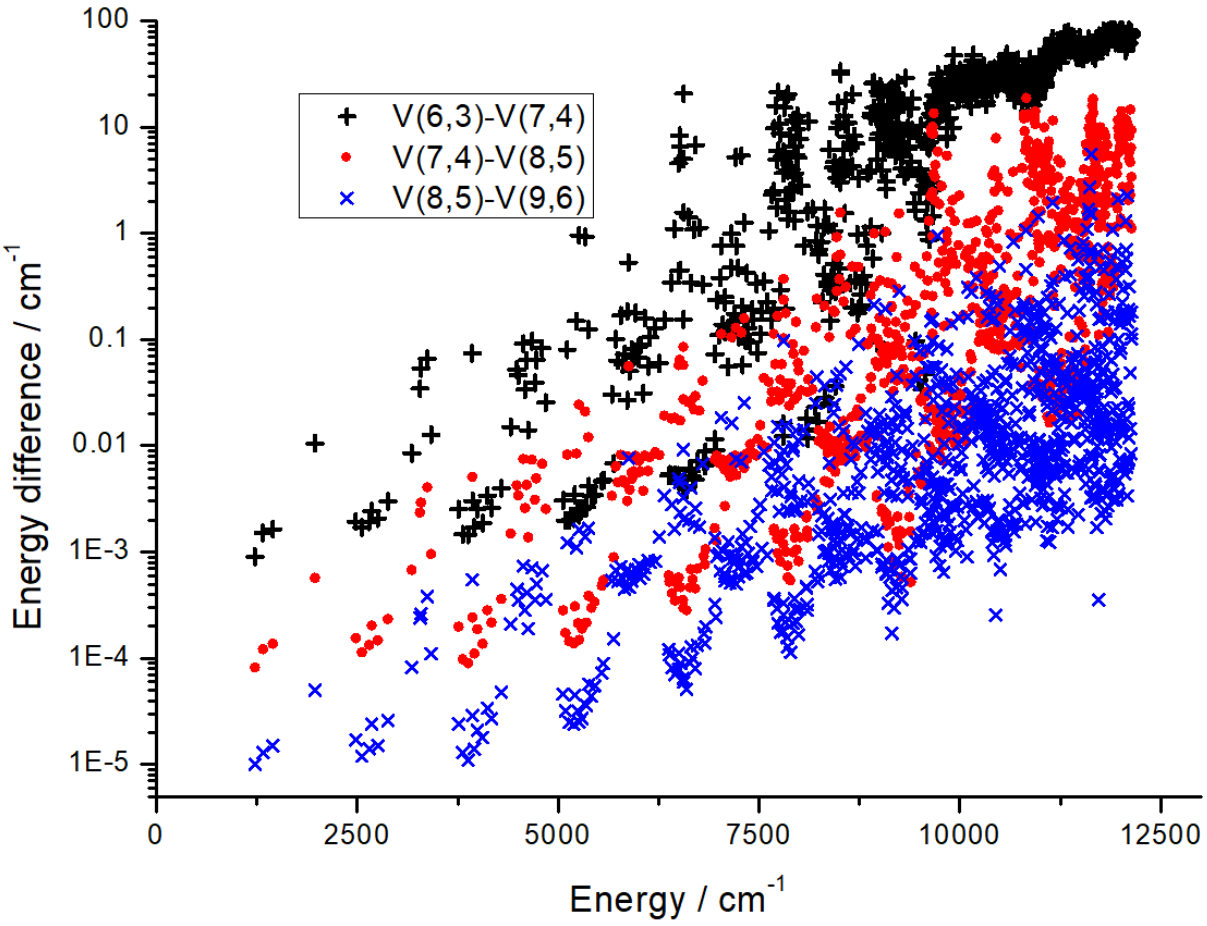

Figure 5. Convergence of vibrational (J=0) energy levels. The radial basis sets V(n,m) contains n radial functions for the CC bond and m radial functions for the CH atom groups.
The differences between radial energy levels calculated for successive numbers of basis functions are depicted with different color codes. The descrepancies between two largest basis sets shown with blue crosses indicate the convergence of the order of 0.1-0.01 cm^{-1} in the vibrational energy range up to about 7500 - 10000 cm^{-1}.

3. Improvement of the electronic basis sets and corrections to the PES

First, we conducted calculations using the augmented core-valence basis set ACV5Z in the whole set of 12047 nuclear geometries. As the next step, we accounted the following *three corrections* to the PES: "mass-velocity-Darwin" (MVD) relativistic corrections, the diagonal Born-Oppenheimer correction (DBOC), and higher-order dynamic electron correlations. The adiabatic DBOC corrections [**92**] [**93**] [**94**] [**95**] [**96**], which make main first-order contributions to the electronic energy beyond the Born-Oppenheimer approximation have been included in accurate PES calculations for several small molecules **([A1]** , [**43**] , [A2], [A3], [**65**], **[76], [78],** [**97**] [**98**] [A4]) , and references therein), but the acetylene molecule was not yet considered.

It has been argued in many previous works [**99**] [**100**] [**101**] [**102**] [**103**] [**104**] that dynamic electron correlations beyond single and double excitations are important to approach spectroscopic accuracy. Such correlations have been included in recent spectroscopically accurate PESs of methane [**76**] [**105**] and a formaldehyde [**77**] [**78**]. A thorough study of the impact of triple and quadruple excitations on the equilibrium geometry and the quartic force field of formaldehyde was reported in [**77**].

In this work, we calculated MVD relativistic corrections with MOLPRO [**88**] [**89**] and DBOC correction with the CFOUR [**106**] program suites on the full reference grid of 12047 nuclear geometries. To check the accuracy of relativistic corrections, DK=4 was also calculated, but the difference between DK and MVD calculations was negligible. DBOC correction is calculated in the cc-pVTZ basis and the accuracy of this calculation does not raise questions [**95**]. Much more expensive and doubtful are calculations for higher-order dynamic electron correlations. The T(Q) correction was calculated with the CFOUR program [**106**] using the noniterative quadruple CCSDT(Q) method [**101**] [**102**] [**103**] [**104**] with the cc-pVTZ one-particle basis and frozen core. The correction term was calculated at 5216 points of two grids of nuclear geometries and approximated by the 4^{th} order expansion of the type (2). Using this form in a way similar to ref [**76**], the energy differences T(Q) were calculated for all other 12047-5216 geometries.

This gave a quite smooth analytical function of all six symmetrized coordinates for the sum of these three corrections:

$$\Delta_{(3corr)}(S_i) = \Delta_{Rel}(S_i) + \Delta_{DBOC}(S_i) + \Delta_{T(Q)}(S_i). \quad (11)$$

In this step we have constructed the *ab initio* corrected surface

$$PES(ACV5Z+3Corr) = PES(ACV5Z) + \Delta_{(3corr)}(S_i). \quad (12)$$

Table 5 provides the energy levels using the PES(ACV5Z) and PES(ACV5Z+3Corr) defined by Eqs.(11, 12) that include the above considered corrections. It is seen that the values of the T(Q) dynamic correction for acetylene are several times higher than those for the methane molecule [**76**] and are of the same order as for formaldehyde [**78**]. The differences between the calculated and measured levels are considerably larger for the ν_2 and ν_4 band origins. Although the PES (ACV5Z + 3Corr) for acetylene is constructed in a similar way to the PES of methane, its accuracy is significantly lower. A similar situation was observed for formaldehyde [**78**]. It was necessary to improve the potential energy surface, particularly along the CC bond. Since the relativistic corrections and DBOC are relatively small, we explored further contributions related to higher-order dynamic electron correlations including quadruple excitations, as well as to the larger, aug-cc-pCV6Z one-particule basis set. To perform this operation, in the next step, we used the iterative CCSDTQ [**103**] [**104**] [**106**] [**107**] method which provides a more rigorous

treatment of dynamic electron correlation corresponding to connected quadruple excitations. However, the calculations that use this method converge very slowly for low-symmetry geometries or for large r_{CC} bond distances. At this level of theory, full PES calculations are extremely demanding, but it was possible to study the corresponding contributions on the most relevant one-dimensional cuts [**76**] [**78**].

In the case of the formaldehyde molecule [**78**], we calculated one-dimensional corrections Δ_Q = CCSDTQ - CCSDT(Q) (cc-pVTZ basis) and Δ_{ACV6Z} = ACV6Z - ACV5Z basis (CCSD(T) method) for 20 geometries. At the first stage, similar one-dimensional corrections were calculated for the acetylene molecule: $\Delta_{QP6}(r_{CC})$, $\Delta_{Q6}(r_{CH})$, and $\Delta_{Q6}(q_{CH})$. The correction Δ_{QP} = CCSDTQP - CCSDT(Q) was evaluated for about 33 points along both bond stretching coordinates. The CCSDTQ(P) - CCSDT(Q) term was calculated in the cc-pVTZ basis, while for CCSDTQP-CCSDTQ(P) the cc-pVDZ basis set was used. The one-dimensional Δ_{ACV6Z} = ACV6Z - ACV5Z corrections were also computed at the same sets of geometries. One-dimensional radial corrections along the CC bond are shown in Figure 6. These corrections result in an increase of the potential energy at distances that exceed r_e(CC). At the distances that are shorter than r_e(CC), the potential energy slightly decreases. For the CC bond, the Δ_Q = CCSDTQ-CCSDT(Q) correction in the cc-pVTZ basis considerably exceeds the Δ_{ACV6Z} = ACV6Z-ACV5Z correction calculated with the CCSD(T) technique.

For the CH bond, the contributions of these corrections are of a similar magnitude. We summarized two corrections $\Delta_{Q+6Z} = \Delta_Q + \Delta_{ACV6Z}$ and approximated this sum analytically using a power series expansion in Morse-type functions Δ_{Q+6Z} (S_1,S_2,S_5) of radial coordinates (2b). The choice of analytical representations had a marginal effect on the vibrational energy levels. The one-dimensional corrections made ν_2 considerably closer to the empirical values, but for the vibrational frequency ν_4, a significant discrepancy remained.

In the case of acetylene, due to the absence of the $f(\tau)^2$ parameter in the PES and the weak dependence of the PES on τ at small angles q, it was impossible to get by with only one-dimensional corrections. A minimum requirement is a 3-dimensional angular correction evaluated at a significant number of points. However, even an approximate shape of the correction surface $\Delta_Q + \Delta_{ACV6Z}$ is not known *a priori*. Therefore, the correction was calculated in a randomized set of points near the minimum of the potential well and approximated by the analytical form (2) up to the third order. The calculation of $\Delta_{Q6}(S_1,S_2,S_3,S_4,S_5,S_6) = \Delta_Q + \Delta_{ACV6Z}$ required considerable computer resources. As quantum-chemical energies were calculated in new geometries, the parameters of series (2) were adjusted. The calculation of 331 points turned out to be sufficient for a reliable determination of the parameters for shape (2)-(4) of the surface Δ_{Q6}. In this case, none of the parameters of the interaction between angular and radial

coordinates was determined. Therefore, in the final version, one-dimensional radial sections were used for the radial part, as in the case of formaldehyde.

One-dimensional potential energy surfaces Δ_{Q6} (q_2) and Δ_{Q6} (q_3) were subtracted by fitting the parameters of the three-dimensional angular surface $\Delta^*_{Q6}(S_3, S_4, S_6) = \Delta_{Q6}(S_3, S_4, S_6) - \Delta_{Q6}(q_2) - \Delta_{Q6}(q_3)$. Note that when fitting the parameters $\Delta^*_{Q6}(S_3, S_4, S_6)$, in addition to 331 randomized geometries, 39 geometries previously obtained for one-dimensional angular sections Q were taken in account. The analytical form of $\Delta^*_{Q6}(S_3, S_4, S_6)$ was adjusted with an RMS deviation of 0.088 cm^{-1}.

This accuracy makes it possible to estimate that the contribution of the determination error of Δ^*_{Q6} to the lower vibrational levels does not exceed 0.3 cm^{-1}. The contribution of Δ_{Q6} brings ν_4 closer to the empirical values. However, the calculated ν_4 levels differ from the empirical values by more than 1.45 cm^{-1}. Table 3 summarizes the contributions of various corrections to vibrational levels and our final ab initio results. The experimental energy levels are collected from papers [**108**], [**109**], [**110**], and [**111**]. Previous experiences in the determination of this type of PES corrections for various molecules showed that corrections evaluated along the stretching of chemical bonds provide the maximum contribution. In the case of the CC bond, the one-dimensional correction P obtained as the difference CCSDTQP-CCSDTQ in the cc-pVDZ basis, calculated with the MRCC program [**112**] turned out to be quite large. Our final ab intio PES that includes these four corrections was constructed as follows:

$$\mathrm{PES(ACV5Z+4Corr)} = \mathrm{PES(ACV5Z)} + \Delta_{(3corr)}(S_i) + \Delta^*_{Q6}(S_3, S_4, S_6) + \Delta_{CC\_QP6}(r_2) + \Delta_{CH\_Q6}(r_1) + \Delta_{CH\_Q6}(r_3) + \Delta_{qHC\_Q6}(q_2) + \Delta_{qHC\_Q6}(q_3) \quad (13)$$

The fourth correction Δ_{Q+6Z} improves the accuracy of the calculated fundamental frequencies and brings them closer to the measured values, especially for ν_2. Also, the correction diminished the calculated value of the equilibrium geometry r_{CCe} . The rCH correction has a noticeably smaller effect on energy levels than the rCC correction.

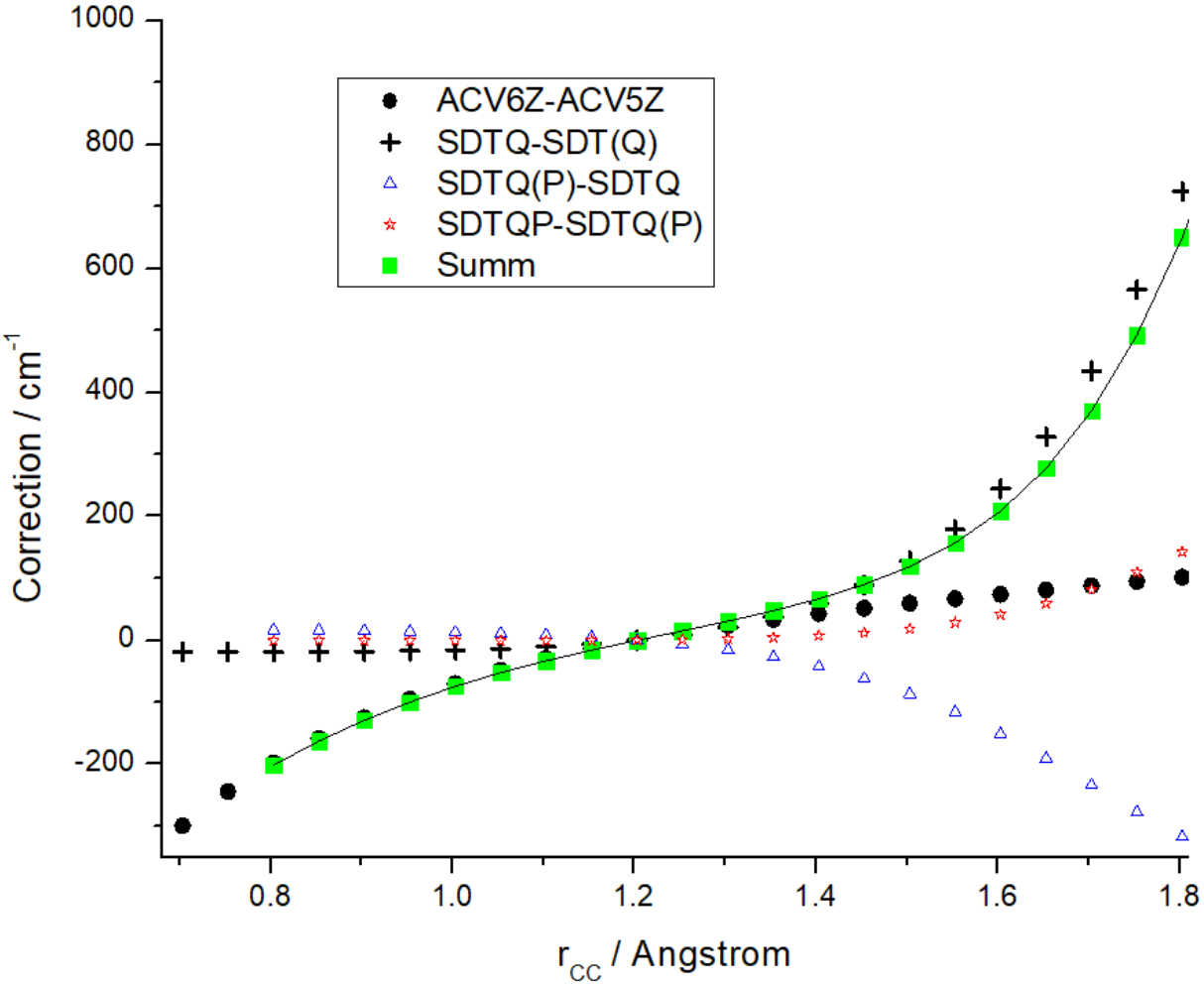

Figure 6 *One-dimensional radial corrections along the CC bond (solid line). The contributions Δ_Q = CCSDTQ - CCSDT(Q) - the rigorous account for connected quadruple excitations in dynamic electron correlation - are depicted with black crosses, while the Δ_{AC6Z} =(ACV6Z-ACV5Z) , Δ_Q = CCSDTQ(P) – CCSDTQ, Δ_P = CCSDTQP - CCSDTQ(P) corrections calculated at the CCSD(T) level are are depicted with circles, triangles and stars, respectively. The sum of all corrections Δ_{Q+P+6Z} = Δ_Q + $\Delta_{(P)}$ + Δ_P+ Δ_{AC6Z} is depicted with solid line.*

As a rule, the caculated origins of the nν_4 bands deviate from observations by values slightly smaller than the product of n and the error in the ν_4 band origin (-1.45cm^{-1}). At the same time, the deviation of other four fundamental frequencies is considerably smaller, the average value being 0.25 cm^{-1}. The large deviation of ν_4 could be explained by the significant contributions of T(Q) and Δ_{Q6}. The contribution of T(Q) is always negative while the contribution of Δ_{Q6} is always positive. In this case, the value of the Δ_{Q6} contribution is greater than half of the T(Q) contribution. A significant part of the Δ_{Q6} contribution is precisely due to the difference Q - (Q). Thus, we can assume that the (P) contribution could be negative, reducing the calculated value of ν_4. In general, it is not clear which factors could significantly increase the value of ν_4.

The maximum contribution to (13) is caused by corrections related to dynamic electron correlation, and they are mainly calculated in the cc-pVTZ basis. Due to their computational

complexity, it is quite difficult to calculate corrections in a larger basis. To assess the possible influence of the basis, we have compared some one-dimensional rCC corrections in the cc-pVTZ and cc-pVDZ basis sets. The comparison showed that the difference in the contribution of the corrections can vary up to 20% when the basis is changed. Reducing the contribution of the T(Q) correction could bring ν_4 closer to the empirical value, but the recalculation of the corrections in the larger cc-pVQZ basis is too expensive, especially for calculations in a full 6-dimensional space. In addition, the QP+6Z correction is also quite significant. This correction can be calculated with a maximum accuracy of 25%. To further improve an accuracy of the C_2H_2 PES, an account of full multy-dimencional corrections would be necessary.

Energy levels calculated from the purely ab initio PES are compared with the empirical values of ref. [**113**] in Table 4 up to the 8-th polyad. The last two colums of Table 4 give also the comparison with calculations using the empirically optimised PESs including two or seven fitted parameters. It can be seen that the PES with two adjustable parameters brings the ν_4 band origin noticeably closer to the empirical value. At the same time, the PES with seven adjustable parameters slightly improves the RMS (calc.-obs.) deviation in comparison with the two-parameters case. Starting from polyad 8, the RMS deviation begins to increase even for the PESs with adjustable parameters. Note that our vibrational assignment is not always in agreement with the identification from work [**113**]. For four empirical levels, including two of the polyad 7, and two of the polyad 8, it was not possible to find calculated levels that have consistent identification.

Table 3. Some J=0,1 lower levels with contributions of relativistic, DBOC corrections, and high-order electron correlations up to 3376 cm^{-1}.

Vib. State	*C*	Emp. levels *	Contributions of corrections #				Theoretical levels with corrections			
			Rel.	DBOC	T(Q)	QP+6Z	ACV5Z	ACV5Z +3corr	ACV5Z +4corr	Exp-Calc##
0 0 0 0 0 0 0 0 1	e	2.353286	0.00	0.00	0.00	0.00	2.35	2.35	2.353372	0.00
0 0 0 1 1 0 0 1 1	f	614.044355	-1.05	0.34	-5.75	2.82	616.25	609.78	612.59791	1.45
0 0 0 1 1 0 0 1 1	e	614.054888	-1.05	0.34	-5.75	2.82	616.26	609.79	612.60838	1.45
0 0 0 0 0 1 1 1 1	e	731.506987	0.30	-0.01	-3.30	1.03	733.61	730.60	731.62343	-0.12
0 0 0 0 0 1 1 1 1	f	731.516374	0.30	-0.01	-3.30	1.03	733.62	730.61	731.63283	-0.12
0 0 0 2 0 0 0 0 0	e	1230.390303	-2.00	0.64	-11.16	4.90	1235.74	1223.22	1228.1242	2.27
0 0 0 2 0 0 0 0 1	e	1232.749162	-2.00	0.64	-11.16	4.90	1238.10	1225.58	1230.483	2.27
0 0 0 1 1 1 -1 0 0	e	1328.073466	-0.81	0.31	-8.96	3.96	1332.55	1323.09	1327.0474	1.03
0 0 0 1 1 1 -1 0 1	e	1330.434308	-0.81	0.31	-8.96	3.96	1334.91	1325.45	1329.4084	1.03
0 0 0 1 1 1 -1 0 0	f	1340.550679	-0.79	0.33	-9.18	3.68	1344.96	1335.32	1338.9995	1.55
0 0 0 1 1 1 -1 0 1	f	1342.911183	-0.78	0.33	-9.18	3.68	1347.32	1337.68	1341.3598	1.55
0 0 0 0 0 0 2 0 0	e	1449.112363	0.58	-0.03	-6.67	1.99	1453.53	1447.41	1449.4051	-0.29
0 0 0 0 0 0 2 0 1	e	1451.474822	0.59	-0.03	-6.68	1.99	1455.89	1449.78	1451.7676	-0.29
0 0 0 3 1 0 0 1 1	e	1856.947677	-2.90	0.92	-16.47	7.01	1865.25	1846.80	1853.8092	3.14
0 0 0 3 1 0 0 1 1	f	1856.968230	-2.90	0.92	-16.47	7.01	1865.27	1846.82	1853.83	3.14
0 0 0 2 2 1 -1 1 1	e	1942.356142	-1.84	0.61	-14.47	6.18	1949.69	1933.99	1940.1677	2.19
0 0 0 2 2 1 -1 1 1	f	1942.371328	-1.84	0.61	-14.47	6.18	1949.70	1934.00	1940.1828	2.19
0 0 0 2 0 1 1 1 1	f	1962.052115	-1.77	0.62	-14.64	5.89	1969.60	1953.82	1959.7053	2.35
0 0 0 2 0 1 1 1 1	e	1962.057447	-1.77	0.62	-14.64	5.89	1969.61	1953.82	1959.7105	2.35
0 1 0 0 0 0 0 0 0	e	1974.316617	0.29	0.04	-7.09	2.12	1978.58	1971.81	1973.9309	0.39
0 1 0 0 0 0 0 0 1	e	1976.656600	0.29	0.04	-7.09	2.12	1980.92	1974.15	1976.2719	0.38
0 0 0 1 1 2 0 1 1	e	2050.232293	-0.57	0.28	-12.25	5.17	2057.06	2044.52	2049.6873	0.54
0 0 0 1 1 2 0 1 1	f	2050.251456	-0.57	0.28	-12.25	5.17	2057.08	2044.54	2049.7064	0.55
0 0 0 1 -1 2 2 1 1	f	2068.152962	-0.53	0.31	-12.60	4.53	2074.97	2062.14	2066.6707	1.48
0 0 0 1 -1 2 2 1 1	e	2068.161538	-0.53	0.31	-12.60	4.53	2074.97	2062.15	2066.679	1.48
0 0 0 0 0 3 1 1 1	e	2171.514343	0.87	-0.04	-10.14	2.87	2178.28	2168.97	2171.8424	-0.33
0 0 0 0 0 3 1 1 1	f	2171.533306	0.87	-0.04	-10.14	2.87	2178.30	2168.99	2171.8615	-0.33
			-3.70	1.16	-21.43	8.75	2497.35	2473.38	2482.1288	
			-3.70	1.16	-21.43	8.75	2499.72	2475.74	2484.493	
0 0 0 3 1 1 -1 0 0	e	2560.594937	-2.73	0.85	-19.47	7.89	2571.18	2549.84	2557.7257	2.87
0 0 0 3 1 1 -1 0 1	e	2562.961453	-2.73	0.85	-19.47	7.89	2573.55	2552.20	2560.0924	2.87
--0 1 0 1 1 0 0 1 1	e	2575.873197	-0.84	0.40	-13.09	5.03	2582.51	2568.98	2574.0152	1.86
0 1 0 1 1 0 0 1 1	f	2575.883903	-0.84	0.40	-13.09	5.03	2582.52	2568.99	2574.0257	1.86
			-2.68	0.89	-19.93	7.84	2594.50	2572.78	2580.6153	
0 0 0 3 1 1 -1 0 1	f	2586.208355	-2.68	0.89	-19.93	7.84	2596.86	2575.14	2582.9806	3.23
0 0 0 2 2 2 -2 0 0	e	2648.014468	-1.64	0.56	-17.58	7.48	2657.79	2639.12	2646.604	1.41
0 0 0 2 2 2 -2 0 1	e	2650.383588	-1.64	0.56	-17.59	7.48	2660.16	2641.49	2648.9731	1.41
			-1.63	0.60	-18.00	7.21	2670.77	2651.74	2658.9475	
0 0 0 2 2 2 -2 0 1	f	2663.556848	-1.63	0.60	-18.00	7.21	2673.14	2654.10	2661.3156	2.24
			-1.56	0.61	-18.20	6.71	2693.90	2674.77	2681.4791	
			-1.55	0.61	-18.20	6.71	2696.27	2677.13	2683.8459	
0 1 0 0 0 1 1 1 1	e	2704.249883	0.58	0.04	-10.60	3.18	2710.74	2700.76	2703.9442	0.31
0 1 0 0 0 1 1 1 1	f	2704.259331	0.58	0.04	-10.60	3.18	2710.75	2700.77	2703.9536	0.31
0 0 0 1 1 3 -1 0 0	e	2757.797907	-0.34	0.25	-15.59	6.12	2767.08	2751.40	2757.5199	0.28
0 0 0 1 1 3 -1 0 1	e	2760.168254	-0.34	0.25	-15.59	6.12	2769.45	2753.77	2759.8905	0.28
			-0.30	0.31	-16.13	5.36	2792.94	2776.82	2782.1796	
0 0 0 1 1 3 -1 0 1	f	2786.022355	-0.30	0.31	-16.13	5.36	2795.31	2779.19	2784.5484	1.47
0 0 0 0 0 4 0 0 0	e	2880.220077	1.13	-0.04	-13.67	3.71	2889.48	2876.90	2880.6153	-0.40
0 0 0 0 0 4 0 0 1	e	2882.592018	1.13	-0.04	-13.67	3.71	2891.85	2879.27	2882.9871	-0.40
0 1 0 1 1 1 -1 0 0	e	3281.899025	-2.57	0.84	-17.44	4.51	3296.16	3276.99	3281.5016	0.40
0 1 0 1 1 1 -1 0 1	e	3284.244150	-2.57	0.84	-15.10	4.51	3296.17	3279.34	3283.8474	0.40
0 0 1 0 0 0 0 0 0	e	3294.839579	-0.35	0.14	-8.87	2.69	3300.99	3291.91	3294.606	0.23
0 0 1 0 0 0 0 0 1	e	3297.184318	-0.35	0.14	-10.52	4.34	3303.34	3292.61	3296.9503	0.23
			-0.58	0.40	-15.08	4.27	3309.51	3294.25	3298.5257	
0 1 0 1 1 1 -1 0 1	f	3302.982999	-0.58	0.40	-16.72	5.91	3311.86	3294.96	3300.8733	2.11
1 0 0 0 0 0 0 0 0	e	3372.838987	0.53	-0.48	-4.44	3.25	3374.30	3369.91	3373.1654	-0.33
1 0 0 0 0 0 0 0 1	e	3375.186841	0.53	-0.48	-6.76	5.58	3376.64	3369.92	3375.5051	-0.32
RMS deviation										

*) Experimental values in wavenumber units (cm^{-1}), from ref [**23**]. *C* is the symmetry type.

#) Rel.= relativistic; T(Q) = CCSDT(Q) – CCSD(T) correlation; QP+6Z = quadruple Δ_{Q+6Z} correction (see the text for explanation).

476 ##) Experimental minus calculated levels corresponding to the full ab initio PES(ACVZ6 + 4Corr).
477
478 **Table 4. Vibrational levels for the $^{12}C_2H_2$ isotopologue up to 8-th polyad.**

Vibr State		Empirical M.Herman et all.*	E"*	Calc	E"-Calc	E"-Calc^{+} 2 adjusted param	E"-Calc^{++} 7 adjusted param
0001100	0,1,1,g	612.871	614.048	612.5976	1.450	0.321	0.212
0000011	0,1,1,u	730.332	731.509	731.6228	-0.114	0.006	0.018
Polyad 1					**1.029**	**0.227**	**0.150**
0002000	0,2,0,g	1230.39	1230.390	1228.123	2.267	0.064	-0.110
0002200	0,2,2,g	1233.52	1235.873	1233.287	2.586	0.354	0.175
000111-1	0,2,0,u1	1328.074	1328.074	1327.046	1.028	0.021	0.122
0001-111	0,2,0,u2	1340.552	1340.552	1338.999	1.553	0.546	0.304
0001111	0,2,2,u	1347.52	1349.873	1348.61	1.263	0.256	0.241
0000020	0,2,0,g	1449.112	1449.112	1449.403	-0.291	-0.057	-0.120
0000022	0,2,2,g	1463.016	1465.369	1465.648	-0.278	-0.039	-0.031
Polyad 2					**1.561**	**0.267**	**0.178**
0003100	0,3,1,g	1855.72	1856.897	1853.808	3.089	-0.162	-0.324
0003300	0,3,3,g	1861.93	1865.460	1861.995	3.465	0.154	-0.043
000221-1	0,3,1,u	1941.179	1942.356	1940.166	2.190	0.088	0.114
0002011	0,3,1,u	1960.874	1962.051	1959.709	2.342	0.261	0.016
0002211	0,3,3,u	1972.56	1976.090	1973.699	2.391	0.285	0.257
0100000	1,3,0,g1	1974.316	1974.316	1973.92	0.396	0.374	0.265
0001-122	0,3,1,g	2049.059	2050.236	2049.685	0.551	-0.337	-0.214
0001120	0,3,1,g	2066.99	2068.167	2066.677	1.490	0.596	0.337
0001122	0,3,3,g	2084.81	2088.340	2087.343	0.997	0.111	0.171
0000031	0,3,1,u	2170.343	2171.520	2171.84	-0.320	0.029	-0.087
0000033	0,3,3,u	2198.09	2201.620	2202.046	-0.426	-0.067	-0.069
Polyad 3					**1.942**	**0.275**	**0.204**
000311-1	0,4,0,u1	2560.6	2560.600	2557.722	2.878	-0.242	-0.127
000331-1	0,4,2,u	2561.526	2563.879	2560.613	3.267	0.090	0.065
0101000****	1,4,1,g	2574.7	2575.877	2574.007	1.869	0.698	0.430
0003-111	0,4,0,u2	2583.845	2583.845	2582.978	0.867	0.124	-0.165
0003111	0,4,2,u	2589.683	2592.036	2588.881	3.155	0.037	-0.126
000222-2	0,4,0,g1	2648.018	2648.018	2646.6	1.418	-0.557	-0.339
0002-222	0,4,0,g2	2661.188	2661.188	2661.313	-0.125	0.259	0.114
0002220	0,4,2,g	2666.151	2668.504	2666.049	2.455	-0.399	-0.258
0100011	1,4,1,u	2703.076	2704.253	2703.936	0.317	0.416	0.287
000113-1	0,4,0,u1	2757.798	2757.798	2757.516	0.282	-0.493	-0.413
0001-133	0,4,2,u	2773.193	2775.546	2775.3	0.246	-0.521	-0.404
0001-131	0,4,0,u2	2783.651	2783.651	2784.546	-0.895	0.680	0.326
0001131	0,4,2,u	2795.5	2797.853	2796.443	1.411	0.629	0.380
0000040	0,4,0,g1	2880.22	2880.220	2880.611	-0.391	0.064	-0.149
0000042	0,4,2,g	2894.069	2896.422	2896.816	-0.393	0.068	-0.089
Polyad 4					**1.723**	**0.421**	**0.276**
010111-1	1,5,0,u1	3281.899	3281.899	3281.467	0.432	-0.159	0.317
0010000	1,5,0,u1	3294.839	3294.839	3294.553	0.286	-0.175	0.337
0101-111	1,5,0,u2	3300.637	3300.637	3298.519	2.118	1.070	0.634
0101111	1,5,2,u	3307.713	3310.066	3308.318	1.749	0.701	0.496
1000000	1,5,0,g1	3372.849	3372.849	3373.099	-0.250	-0.264	0.617
0100020	1,5,0,g1	3420.388	3420.388	3420.235	0.153	0.367	0.142
0100022	1,5,2,g	3434.113	3436.466	3436.276	0.190	0.410	0.246
Polyad 5					**1.065**	**0.543**	**0.435**
000511-1	0,6,0,u1	3818.44	3818.440	3813.835	4.605	-0.456	-0.067
000531-1	0,6,2,u	3820.24	3822.593	3817.577	5.016	-0.099	0.183
000511-1	0,6,0,u2	3850.32	3850.320	3845.604	4.716	-0.306	-0.391
000511-1	0,6,2,u	3855.82	3858.173	3853.419	4.754	-0.285	-0.287
0011100	1,6,1,u	3882.41	3883.587	3881.789	1.798	0.051	0.355
0011100	1,6,1,u	3898.34	3899.517	3897.966	1.551	-0.007	0.409
0200000	2,6,0,g1	3933.897	3933.897	3935.481	-1.584	0.699	0.466
1001100	1,6,1,g	3970.05	3971.227	3970.284	0.943	-0.153	0.611
0010011	1,6,1,g	4002.44	4003.617	4003.213	0.404	-0.206	0.152
0010011	1,6,1,g	4016.71	4017.887	4017.929	-0.042	-0.342	0.227
1000011	1,6,1,u	4092.345	4093.522	4094.005	-0.483	-0.377	0.487

0100031	1,6,1,u	4140.055	4141.232	4141.102	0.130	0.459	0.159
Polyad 6					**2.896**	**0.344**	**0.353**
010311-1	1,7,0,u1	4488.85	4488.850	4486.399	2.451	-0.287	0.055
0012000	1,7,0,u1	4489.05	4489.050	4486.399	2.651	-0.087	0.255
010331-1	1,7,2,u	4490.81	4493.163	4490.203	2.961	0.088	0.262
010331-1	1,7,2,u	4490.96	4493.313	4490.203	3.111	0.238	0.412
0012000	1,7,0,u1	4508.03	4508.030	4505.628	2.402	-0.256	0.110
0012200	1,7,2,u	4509.21	4511.563	4508.999	2.564	-0.062	0.300
0102200	1,7,2,u	4509.81	4512.163	***			
0103-111	1,7,0,u2	4521.07	4521.070	4517.304	3.766	0.593	0.025
0103111	1,7,2,u	4527.25	4529.603	4525.748	3.855	0.678	0.259
0102-222	1,7,0,g2	4599.78	4599.780	4597.798	1.982	0.336	0.433
0102220	1,7,2,g	4608	4610.353	4608.67	1.684	-0.120	0.136
001111-1	1,7,0,g1	4609.33	4609.330	4608.486	0.844	-0.564	0.159
0011-111	1,7,0,g2	4617.92	4617.920	4616.325	1.595	0.182	0.468
0011111	1,7,2,g	4624.79	4627.143	4625.984	1.159	-0.221	0.368
010311-1	1,7,0,u1	4658.31	4658.310	***			
100111-1	1,7,0,u1	4673.63	4673.630	4673.163	0.467	-0.486	0.430
1001-111	1,7,0,u1	4688.84	4688.840	4687.739	1.101	0.064	0.666
1001111	1,7,2,u	4692.06	4694.413	4693.761	0.652	-0.268	0.551
010113-1	1,7,0,u1	4710.74	4710.740	4710.405	0.335	-0.265	-0.049
0101-133	1,7,2,u	4725.85	4728.203	4727.846	0.357	-0.227	0.040
0010020	1,7,0,u1	4727.06	4727.060	4727.523	-0.463	-0.535	0.100
0010022	1,7,2,u	4741.04	4743.393	4743.575	-0.181	-0.355	0.215
1000020	1,7,0,g1	4800.14	4800.140	4800.96	-0.820	-0.599	0.153
1000022	1,7,2,g	4814.2	4816.553	4817.338	-0.785	-0.561	0.270
Polyad 7					**1.998**	**0.374**	**0.313**
0008200	0,8,2,g	5068.8	5071.153	***			
0008000	0,8,0,g1	5068.8	5068.800	5061.242	7.558	-0.268	0.570
0008000	0,8,0,g1	5069.72	5069.720	***			
000711-1	0,8,0,u1	5098.38	5098.380	5092.639	5.741	-1.067	-0.158
000731-1	0,8,2,u	5100.92	5103.273	5097.153	6.120	-0.745	0.073
0013100	1,8,1,u	5102.79	5103.967	5100.69	3.276	-0.474	-0.101
0013100	1,8,1,u	5124.587	5125.764	5122.425	3.339	-0.373	-0.017
0007-111	0,8,0,u2	5137.37	5137.370	5131.254	6.116	-0.610	-0.292
0007111	0,8,2,u	5142.63	5144.983	5138.981	6.003	-0.745	-0.363
000513-1	0,8,0,u1	5198.86	5198.860	5194.406	4.454	-0.409	0.382
0006020	0,8,2,g	5221	5223.353	5218.929	4.424	-1.311	-1.246
0005131	0,8,2,u	5226.7	5229.053	5223.751	5.302	0.502	0.999
020111-1	2,8,0,u1	5230.022	5230.022	5228.695	1.327	0.334	0.180
000533-3	0,8,0,u1	5254.53	5254.530	5249.095	5.435	0.660	0.694
0110000	2,8,0,u1	5260.002	5260.002	5260.117	-0.115	-0.241	0.655
0005-133	0,8,2,u	5262.39	5264.743	5258.63	6.113	1.330	1.481
100221-1	1,8,1,u	5269.729	5270.906	5269.678	1.227	-0.712	0.145
100221-1	1,8,1,u	5290.283	5291.460	5289.941	1.519	-0.398	0.172
0005-131	0,8,0,u2	5298.93	5298.930	5293.306	5.624	0.879	0.625
1002011	1,8,1,u	5302.4	5303.577	5302.19	1.386	-0.505	-0.181
0005131	0,8,2,u	5306.06	5308.413	5303.329	5.084	0.342	0.177
1100000	2,8,0,g1	5335.549	5335.549	5335.422	0.127	0.092	0.919
1001120	1,8,1,g	5382.738	5383.915	5383.948	-0.034	-0.843	0.041
1000031	1,8,1,u	5510.59	5511.767	5512.483	-0.717	-0.382	0.280
Polyad 8					**4.384**	**0.682**	**0.597**
RMS deviation**					**2.719**	**0.462**	**0.387**

*) Empirical levels from ref. [**113**] in cm^{-1}. E" levels are empirical levels plus B_0*J (B_0=1.1764632cm-1)

**) RMS deviation without four levels.

***) Four calculated levels are missing from the table because of a wrong assignment in ref. [**113**]. The level (0102200 1,7,2,u) has wrong wavenumber 4509.81 cm^{-1}. Level 010311-1 1,7,0,u1 also has wrong wavenumber 4658.31 cm^{-1}. Level 0008000 0,8,0,g1 appears twice. Probably, level 0008200 0,8,2,g has wrong wavenumber.

****) Wrong energy level identification

4. Splitting for (e – f) doublets in rovibrational energies

It is known that the rotational patterns of Σ, Π, Δ, and Φ vibrational states form (e-f) near degenerate doublets - closely lying levels of different parity with respect to inversion. Despite the limited accuracy of the PES, the use of the exact kinetic energy makes it possible to calculate the splitting in (e – f) doublets and determine its *J*-dependence with high accuracy. The symmetry-reduced basis set can be represented as:

$$\left|J,M,\sigma,p,l_1,m_1,l_2,m_2\right\rangle \equiv (-1)^{m_1}\frac{\left(\left|J,M,p,l_1,m_1,l_2,m_2\right\rangle+(-1)^{\sigma+p}\left|J,M,p,l_2,m_2,l_1,m_1\right\rangle\right)}{\sqrt{2\left(1+\delta_{m_1+m_2,0}\delta_{l_1l_2}\right)}} \quad (14)$$

Here $\left|J,M,p,l_1,m_1,l_2,m_2\right\rangle$ is defined by formula (8), p – is the parity with respect to inversion: $E^*\left|p,\sigma\right\rangle=(-1)^p\left|p,\sigma\right\rangle$, and σ – is the parity with respect to permutation of a pair of indices $(l_1,m_1)\leftrightarrow(l_2,m_2)$ in eigenfunctions (10): $\hat{\sigma}\left|p,\sigma\right\rangle=(-1)^{\sigma}\left|p,\sigma\right\rangle$. This definition was not commonly used in previous works, but it is convenient for the software implementation, since it does not depend on *J*. In the conventional notations, the blocks with even $p+\sigma$ are denoted by *g* and correspond to even n_3+n_5 values. The blocks with odd $p+\sigma$ are denoted by *u* and correspond to odd n_3+n_5 values. For each vibrational band, the parity *g* or *u* is defined by the number *mod(n_3+n_5, 2).*

The complete space of basis functions is divided into four independent blocks having even or odd values of p,σ. In the *J = 0* case the basis set is orthogonal, but in a general case with J > 0, the basis set (11) is non-orthogonal. Note that for $m_1+m_2>0$, the function $\left|J,M,p,l_1,m_1,l_2,m_2\right\rangle$ always contain two components $\left|J,M,l_1,m_1,l_2,m_2\right\rangle$. The set of basis functions includes all possible functions of the form (14) such that $l_1+l_2\le L_{max}$ [**84**].

Let us first consider the case *J = 0*. Each of the basis functions $\left|J,M,\sigma,p,l_1,m_1,l_2,m_2\right\rangle$ can include combinations of 1, 2 or 4 functions $\left|J,M,l_1,m_1,l_2,m_2\right\rangle$ defined by Eq.(6). The number of basis functions containing 4 components $\left|J,M,l_1,m_1,l_2,m_2\right\rangle$ is the same in each block.

The block $p=0,\sigma=0$ is the only block, for which basis functions contain one component. In the case $p=1,\sigma=1$, all basis functions contain 4 components. The bocks $p=1,\sigma=0$, and $p=0,\sigma=1$ contain the same number of functions with two components, but these functions themselves are different. In the case $p=1,\sigma=0$, the functions have the form $\left(Y_{l_1 0}(\theta_1,\varphi_1)Y_{l_2 0}(\theta_2,\varphi_2)-Y_{l_2 0}(\theta_1,\varphi_1)Y_{l_1 0}(\theta_2,\varphi_2)\right)/\sqrt{2}$, and their amount is equal to $\sum_{l_1>l_2}^{L_{max}}\sum_{l_2\ge 0}^{L_{max}}1=L_{max}(L_{max}+1)/2$. In the case $p=0,\sigma=1$, the functions have the form $\left(Y_{l_1,-m}(\theta_1,\varphi_1)Y_{l_1,m}(\theta_2,\varphi_2)+Y_{l_1 m}(\theta_1,\varphi_1)Y_{l_1 -m}(\theta_2,\varphi_2)\right)/\sqrt{2}$, and their amount is also equial to $\sum_{l=1}^{L_{max}}\sum_{m=1}^{l}1=L_{max}(L_{max}+1)/2$. Since the basis fubctions in each of the four blocks p,σ are

different, the energy levels in different blocks are not degenerate (except for possible accidental coincidence) at $J = 0$. If we remove the Coriolis interaction term

$H_{corr} = \frac{1}{2M\mu_R R^2}\left[\left(\hat{l}_2^- + \hat{l}_1^-\right)\hat{\hat{J}}^- - \left(\hat{l}_2^+ + \hat{l}_1^+\right)\hat{\hat{J}}^+\right]$ from the Hamiltonian (7), then all levels of a certain vibrational state in the block $J + p = 1$ would coincide exactly with the levels in the block $J + p = 0$ for $K > 0$. In this case, it really makes sense to talk about the point group $D_{\infty h}$ [**37**], [**40**], for which doubly degenerate representations K $(K=1,\ldots\infty)$ would occur. But this scenario is only true in an approximation where the Coriolis interaction H_{corr} is neglected. In reality, due to the weak Coriolis interaction between the $K = 1$ and $K = 0$ states, the $J = 1$ levels in doublets are shifted differently in each of the blocks p,σ. Since the Coriolis interaction in our approach is described by a simple exact KEO, the magnitude of the corresponding (e-f) splitting and its J-dependence are modeled with high accuracy. Note that the absolute accuracy of the levels is much lower as it is limited by the accuracy of the PES. Similarly, the levels with higher values K=2, K=3 etc are also splitted due to the Coriolis interactions. Though K is not an exact quantum number, the contribution of the basis functions with a certain K value is, as a rule, dominant for the wavefuctions of low-lying states. Eigenfunctions with dominant contribution of large K contain insignificant amplitudes of the basis functions with $K = 0$. The higher is K, the smaller is the splitting. But even for large values of K the vibrational-rotational energy levels are always non-degenerate. This behavior is caused by weak Coriolis interaction. Figure 7 shows a diagram of the J = 3 angular matrix elements. The complete wave function consists of 4 blocks of the basis functions with different ($m_1 + m_2$).

$m_1+m_2=0$	**C_{01}**	**0**	**0**
C_{01}	**$m_1+m_2=1$**	**C_{12}**	**0**
0	**C_{12}**	**$m_1+m_2=2$**	**C_{23}**

0	**0**	**C_{23}**	**$m_1+m_2=3$**

Figure 7. Scheme of corner matrix elements for J=3. The basis is formed by eigenfunctions for each m_1+m_2. Nonzero matrix elements occur for the functions of neighboring blocks.

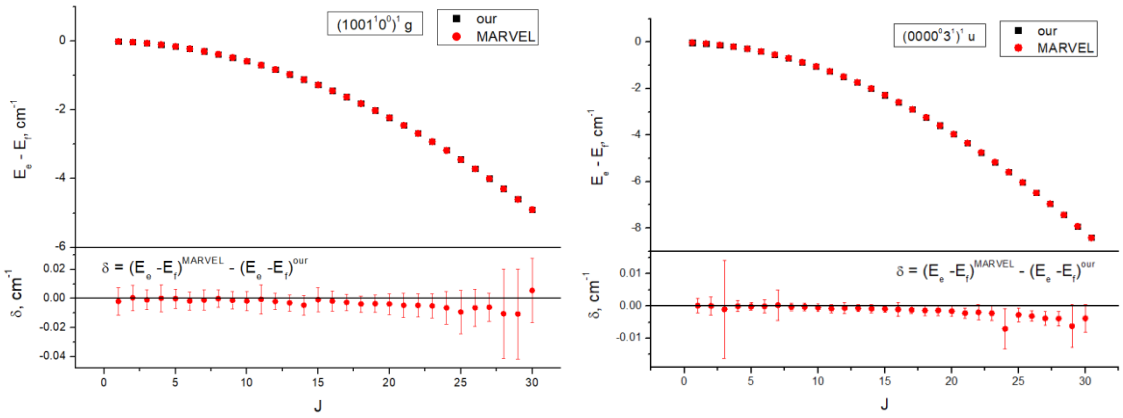

Figure 8. Comparison of the *J*-dependence of (e-f) splittig for the states $(1001^10^0)^1_g$ (left) and $(0000^03^1)^1_u$ (right) between our calculated and empirical values reported by MARVEL study [23]. At the scale of the upper panes, our theoretical values depicted with square, and empirical MARVEL values depicted with red circles nearly coinside. At the blown up scale of the lower panes the difference δ = (MARVEL – theoretical) is depicted by circles on the lower panel with the estimated uncertainty of empirical values shown as the error bars.

Figure 8 shows the energy levels values for the bands $(1001^10^0)^1_g$ and $(0000^03^1)^1_u$ calculated in this work and the empirical values [23] determined using MARVEL procedure [A4]. It can be seen that our calculation describes the splitting of *e* and *f* levels with high accuracy. As a rule, for the most of vibrational bands, the calculated and empirical levels, as well as the levels splitting, look similar and are described by smooth curves. But for some bands, the difference looks like a broken line. For example, Figures 9 and Fifure 10 show the J-dependence of the splittings for the Π states and the Δ states. One of the reasons for the erratic behaviour could be possible misassignments of some levels in experimental works. The irregular splitting often correlates with poor uncertainty of empirical level included in MARVEL database [**23**] . Thus, variational

560 calculation can be useful for testing empirical values of energy levels. [**23**]

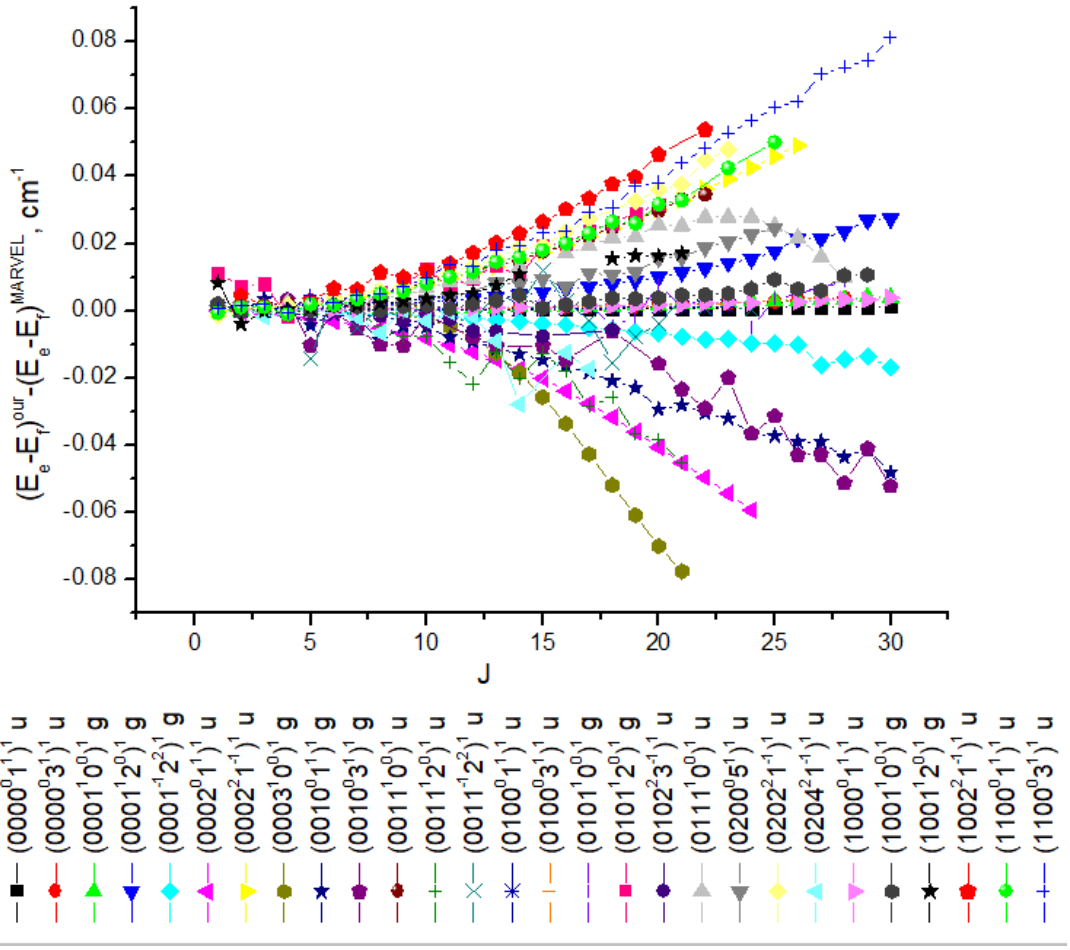

561

562 Figure 9. Differences of the (e-f) splittings predicted in the present study and the MARVEL database
563 [23], for selected Π type states (K = 1).

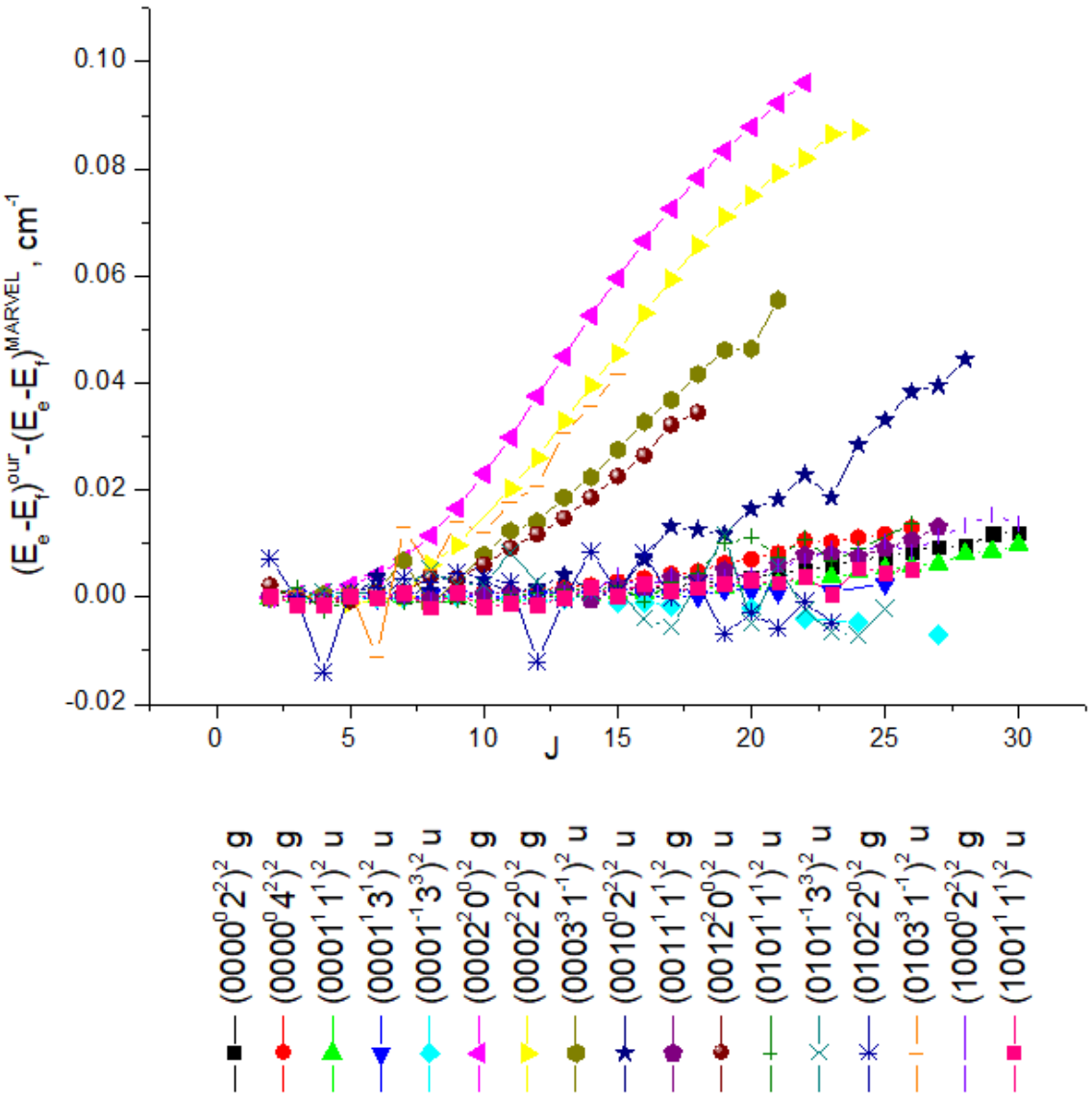

Figure 10. Differences of the (e-f) splittings predicted in the present study and the MARVEL database [23], for selected Δ type states (K = 2).

As a rule, the *J*-dependence of the splittings is well approximated by a third-order polynomial. To estimate the accuracy of the model, we fitted the difference between the (e-f) splittings from MARVEL and our calculation. Table 5 shows the differences between the calculated and empirical splittings as a power function $y = C_0 + C_1 x + C_2 x^2 + C_3 x^3$. For the Σ bands, the shift is large, and it is calculated inaccurately (large coefficient C_0) since the shift depends on the PES. But at the same time, the J dependence of the calculated shift of Σ bands is correct (small coefficients C_1, C_2, C_3). For the Π, Δ, and Φ bands, the difference is small, the J dependence is weak and is well described by polynomials up to the third order.

Table 5. The differences between the empirical and calculated splittings presented as an expansion to the third order in cm^{-1}.

Energy E, cm^{-1}		State	C_0	C_1	C_2	C_3	RMS, cm^{-1}	Adj. R-Square	# of Points	J removed from fit
1328.073466	Σ	$(0001^{1}1^{-1})^{0}$ u	0.18086(14)	0.000012(40)	0.0000038(31)	-0.000000487(69)	0.00020	0.99429	31	
2757.797907	Σ	$(0001^{1}3^{-1})^{0}$ u	0.73712(24)	-0.000130(39)	0.0000099(14)		0.00018	0.95786	19	1,3,12
4673.631058	Σ	$(1001^{1}1^{-1})^{0}$ u	0.25624(73)	-0.000138(113)	-0.0000181(36)		0.00137	0.95042	31	
6623.139603	Σ	$(1101^{1}1^{-1})^{0}$ u	0.88059(98)	0.000578(302)	-0.0001100(249)	-0.00000151(58)	0.00099	0.99856	25	
731.506987	Π	$(0000^{0}1^{1})^{1}$ u	0.000028(105)	0.000011(27)	0.0000000(19)	0.000000034(39)	0.00009	0.9361	29	
2171.514343	Π	$(0000^{0}3^{1})^{1}$ u	0.000045(120)	-0.000031(18)	0.00000581(61)		0.00017	0.97627	26	3,24,29,30
614.044355	Π	$(0001^{1}0^{0})^{1}$ g	0.0000089(893)	0.000014(25)	0.0000031(18)	0.000000031(39)	0.00010	0.99263	30	
2050.232293	Π	$(0001^{1}2^{0})^{1}$ g	-0.000257(417)	0.00018(11)	0.0000001(85)	0.00000086(18)	0.00047	0.99655	30	
2068.161538	Π	$(0001^{-1}2^{2})^{1}$ g	0.000095(743)	-0.000047(204)	-0.000011(15)	-0.00000020(32)	0.00083	0.96951	30	
1962.057447	Π	$(0002^{0}1^{1})^{1}$ u	-0.000676(465)	0.00027(16)	-0.000096(15)	-0.00000077(38)	0.00044	0.99935	24	
1942.356142	Π	$(0002^{2}1^{-1})^{1}$ u	-0.000030(104)	0.000051(33)	0.000077(28)	-0.000000233(68)	0.00011	0.99995	26	
4017.877611	Π	$(0010^{0}1^{1})^{1}$ g	0.00024(154)	0.00032(42)	-0.000119(32)	0.00000190(67)	0.00173	0.98609	30	
3899.504045	Π	$(0011^{1}0^{0})^{1}$ u	0.000378(389)	-0.000004(143)	0.000086(14)	-0.00000062(41)	0.00034	0.99884	22	
2704.249883	Π	$(0100^{0}1^{1})^{1}$ u	-0.000099(39)	0.0000542(29)			0.00009	0.94204	23	
4141.222136	Π	$(0100^{0}3^{1})^{1}$ u	0.00055(28)	-0.000065(47)	0.0000064(16)		0.00043	0.81948	26	
4003.600972	Π	$(0101^{1}2^{0})^{1}$ g	0.0093(23)	-0.00172(50)	0.000147(23)		0.00285	0.89821	20	
7512.125734	Π	$(0200^{0}5^{1})^{1}$ u	0.00008(116)	0.00016(38)	0.0000097(334)	0.00000092(84)	0.00112	0.97459	24	
5819.194833	Π	$(0202^{2}1^{-1})^{1}$ u	-0.00170(91)	0.00058(30)	0.000042(29)	0.00000113(78)	0.00072	0.99721	21	
4093.511896	Π	$(1000^{0}1^{1})^{1}$ u	0.00030(12)	-0.0000080(172)	0.0000040(5)		0.00014	0.97666	30	1,3,10,25
3971.220032	Π	$(1001^{1}0^{0})^{1}$ g	-0.00132(58)	0.000315(34)			0.00143	0.7568	30	30
5270.885653	Π	$(1002^{2}1^{-1})^{1}$ u	0.0022(11)	-0.000095(212)	0.0001127(87)		0.00111	0.99398	19	1,4
6054.402350	Π	$(1100^{0}1^{1})^{1}$ u	-0.00086(100)	0.00020(33)	0.000064(29)	0.00000036(75)	0.00097	0.99454	23	
7468.787187	Π	$(1100^{0}3^{1})^{1}$ u	0.0019(11)	-0.00077(31)	0.000174(23)	-0.00000203(48)	0.00125	0.99737	30	
1465.378177	Δ	$(0000^{0}2^{2})^{2}$ g	0.00051(30)	-0.000183(77)	0.0000130(54)	0.00000021(11)	0.00026	0.995	29	
2896.436694	Δ	$(0000^{0}4^{2})^{2}$ g	0.00062(55)	-0.000303(81)	0.0000309(26)		0.00046	0.98771	22	2,3,7
1349.881320	Δ	$(0001^{1}1^{1})^{2}$ u	-0.00013(18)	0.000046(46)	-0.0000075(33)	0.000000568(67)	0.00015	0.99686	29	
2775.559135	Δ	$(0001^{1}3^{1})^{2}$ u	0.00031(31)	-0.000099(51)	0.0000066(18)		0.00030	0.75369	21	22
1235.874392	Δ	$(0002^{2}0^{0})^{2}$ g	0.0091(12)	-0.00582(39)	0.000967(37)	-0.0000238(10)	0.00072	0.99947	21	
2563.894400	Δ	$(0003^{3}1^{-1})^{2}$ u	-0.00029(219)	-0.00059(44)	0.000157(19)		0.00223	0.9834	19	
4743.370547	Δ	$(0010^{0}2^{2})^{2}$ u	0.00002(272)	0.000074(741)	-0.000019(56)	0.0000027(12)	0.00217	0.97188	27	
4627.107147	Δ	$(0011^{1}1^{1})^{2}$ g	0.00038(105)	-0.00017(29)	0.0000094(229)	0.00000050(52)	0.00080	0.95238	26	
4511.583389	Δ	$(0012^{2}0^{0})^{2}$ u	0.00303(88)	-0.00154(20)	0.0001872(98)		0.00078	0.99478	17	
4816.554911	Δ	$(1000^{0}2^{2})^{2}$ g	0.00010(107)	-0.00022(28)	0.000022(19)	0.000000068(401)	0.00092	0.96016	29	
4694.404604	Δ	$(1001^{1}1^{1})^{2}$ u	-0.00039(89)	-0.00012(14)	0.0000127(50)		0.00110	0.71164	25	
2201.641273	Φ	$(0000^{0}3^{3})^{3}$ u	0.00020(21)	-0.000027(12)			0.00045	0.15048	26	27,28
2088.358695	Φ	$(0001^{1}2^{2})^{3}$ g	0.00087(75)	-0.000100(42)			0.00164	0.15186	27	30

93 sets of differences for e and f vibrational-rotational energy levels of the acetylene molecule were considered when compiling Table 5. Some of these bands are shown in Figures 9, 10, and also in the Supplementary material files. Each group consists of a set of differences between e and f levels for different values of the total angular momentum J (our calculations of the VR energy levels of the acetylene molecule were carried out for values $0 \le J \le 30$). These 93 groups consisted of: 9 difference sets with K = 0 (Σ state), 47 difference sets with K = 1 (Π state), 26 difference sets with K = 2 (Δ state), and 11 difference sets with K = 3 (Φ state). Not all considered sets were used while compiling Table 5.

A smoothness of the *J*-dependence can be visualized using the second derivatives of (E_e-E_f) with respect to *J* computed by the finate difference method. The situation is quite different depending on the vibrational state. Figure 11 shows two examples of the behaviour of these second derivatives versus *J* for our calculates splittings and for empirical MARVEL values [23].

At the left-hand side of Figure 11 for the $(0001^11^1)^2_u$ state, both derivatives are smooth, except for a small feature in the interval *J*=25-28 for the empirical curve. The error bars at the lower pane of this figure show that empirical splitting are quite accurate whereas the theoretical values are somewhat overestimated. At the right-hand side of Figure 11 for the $(1000^00^1)^1_u$ state, the theoretical derivative is still smooth, whereas the empirical ones are erratic with much larger error bars for the empirical splittings.

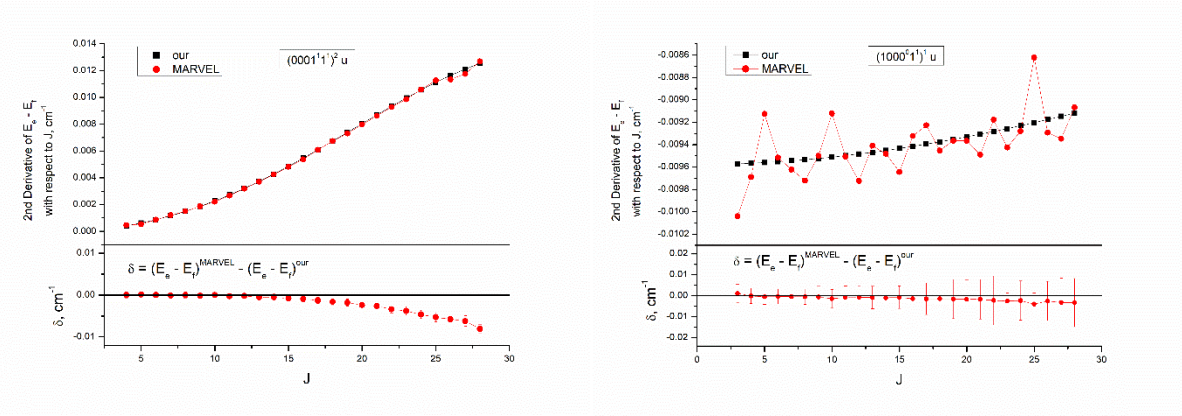

Figure 11. The second derivatives (E_e-E_f) with respect to *J* for the states $(0001^11^1)^2_u$ (left) and $(1000^00^1)^1_u$ (right). At the upper panes of the figures, the theoretical values are depicted with square, and the empirical MARVEL values [23] are depicted with red circles. At the blown up scale of the lower panes the difference δ = (MARVEL – theoretical) is depicted by circles on the lower panel with the estimated uncertainty of empirical values shown as the error bars.

5. Calculations for the C_2D_2 and $^{13}C_2H_2$ isotopologues

The vibrational levels of C_2D_2 given in Table 6 were calculated with nuclear masses using both ab initio and empirically fitted PESs. The calculation Calc(C_2D_2) corresponds to our best ab initio PES(ACV5Z+4Corr) + ΔDBOC, while Calc++(C_2D_2) corresponds to the empirically optimized PES (7 adjusted parameters) fitted to 120 vibrational levels of the main acetylene isotopologue as described in the previous section. The contribution of ΔDBOC was considered as the difference between DBOC for $^{12}C_2D_2$ and $^{12}C_2H_2$. The C_2D_2 isotopologue is heavier than $^{12}C_2H_2$, thus the DBOC correction for C_2D_2 is expected to be less important than this correction for $^{12}C_2H_2$. To calculate the contribution of the ΔDBOC, we expressed it in the form of a fourth-

order Taylor expansion. Experimental levels were taken from work [**113**]. Note that work [**113**] reports only pure vibrational levels. In order to obtain rovibrational levels, we add the value B_0*J, where rotational constants B_0 are well known from analyses of experimental spectra: B_0 = 0.8475 cm^{-1} for C_2D_2 and B_0 = 1.1195 cm^{-1} for $^{13}C_2H_2$. As for the main isotopologue, the energy levels calculated from ab initio PES have large deviations for all ν_4 overtones. Note that our calculated levels C_2D_2 unambiguously correspond to experimental levels in all cases except for $4\nu_5$ and $5\nu_5$.

The vibrational levels of $^{13}C_2H_2$ given in Table 7 were also calculated with nuclear masses using both ab initio and empirically fitted PESs. The comparison of the DBOC parameters for the two isotopologues shows that the contribution of DBOC for $^{13}C_2H_2$ is about 90-95% of that for $^{12}C_2H_2$. The DBOC effect being weak, the accordingly scaled contribution of the main isotopologue (see the respective column of Table 3) could be applied to the calculated $^{13}C_2H_2$ levels. For the $3\nu_3$ level, it is not possible to find a one-to-one correspondence between the empirical and calculated energy levels, most likely due to differences in the assignments. The last rows of Tables 6 and 7 give the RMS deviations between experimental and calculated levels. In both cases, the main contribution to the error in the energy levels calculated from the ab initio PES is caused by the ν_4 overtones.

Table 6. Vibrational levels of the C_2D_2 isotopologue up to 6500 cm^{-1}, in cm^{-1} units.

Vibr State		Empirical*	E" *	Calc	E"-Calc	E"-Calc++ 7 adjusted param
0001100	0,1,1,g	511.532	512.380	510.9645	1.415	0.294
0000011	0,1,1,u	538.636	539.484	539.3923	0.091	0.098
0002000	0,2,0,g	1024.81	1024.810	1022.521	2.289	0.171
000111-1	0,2,0,u	1041.49	1041.490	1040.099	1.391	0.305
0001-111	0,2,0,u	1048.66	1048.660	1048.8	-0.140	0.460
0000020	0,2,0,g	1070.86	1070.860	1070.86	0.000	-0.017
000221-1	0,3,1,u	1552.75	1553.598	1551.168	2.429	0.343
0002011	0,3,1,u	1562.43	1563.278	1560.912	2.365	0.345
0001-122	0,3,1,g	1574.82	1575.668	1574.387	1.281	0.206
0001-122	0,3,1,g	1585.38	1586.228	1584.628	1.599	0.499
0000031	0,3,1,u	1604.54	1605.388	1605.346	0.042	0.022
0100000	1,0,0,g	1764.796	1764.796	1764.757	0.039	-0.132
0000040	0,4,0,g	2136.81	2136.810	2132.263	4.547**	4.440**
0101100	1,1,1,g	2272.401	2273.249	2271.788	1.460	0.183
0100011	1,1,1,u	2305.079	2305.927	2305.649	0.277	0.136
0010000	1,0,0,u	2439.244	2439.244	2439.526	-0.282	0.010
0000051	0,4,1,g	2659.35	2660.198	2663.045	-2.847**	-3.116**
1000000	1,0,0,g	2705.160	2705.160	2705.174	-0.014	-0.089
0102000	1,2,0,g	2783.132	2783.132	2780.78	2.352	0.119
010111-1	1,2,0,u	2803.959	2803.959	2802.443	1.516	0.297
0101-111	1,2,0,u	2811.050	2811.050	2809.222	1.828	0.591
0100020	1,2,0,g	2838.692	2838.692	2838.556	0.136	0.009
0011100	1,1,1,u	2945.17	2946.018	2944.963	1.055	0.361
0010011	1,1,1,g	2972.70	2973.548	2973.748	-0.201	0.198

1001100	1,1,1,g	3201.98	3202.828	3200.842	1.985	0.840
1000011	1,1,1,u	3235.61	3236.458	3236.265	0.193	0.170
0012000	1,2,0,u	3452.35	3452.350	3450.83	1.520	-0.038
001111-1	1,2,0,g	3469.417	3469.417	3468.604	0.813	0.259
0010020	1,2,0,u	3499.72	3499.720	3500.166	-0.446	0.026
0200000	2,0,0,g	3520.812	3520.812	3520.808	0.004	-0.339
1000020	1,2,0,g	3759.38	3759.380	3759.412	-0.032	-0.015
0013100	1,3,1,u	3965.21	3966.058	3962.639	3.418	1.099
0110000	2,0,0,u	4190.638	4190.638	4191.339	-0.701	-0.570
1000031	1,3,1,u	4284.75	4285.598	4285.445	0.152	0.236
0111100	2,1,1,u	4692.77	4693.618	4692.995	0.623	-0.214
0110011	2,1,1,g	4725.68	4726.528	4727.013	-0.486	-0.224
0020000	2,0,0,g	4848.786	4848.786	4850.489	-1.703	-1.130
1010000	2,0,0,u	5097.195	5097.195	5098.321	-1.126	-0.903
0112000	2,2,0,u	5197.800	5197.800	5196.315	1.485	-0.186
0020011	2,1,1,u	5377.375	5378.223	5377.363	0.860	-0.493
2000000	2,0,0,g	5386.456	5386.456	5386.253	0.203	-0.012
110111-1	2,2,0,u	5466.740	5466.740	5465.548	1.192	-0.053
1011100	2,1,1,u	5587.640	5588.488	5588.469	0.019	-0.705
1010011	2,1,1,g	5622.42	5623.268	5623.154	0.114	-0.736
2000011	2,1,1,u	5908.457	5909.305	5908.658	0.646	-0.018
110221-1	2,3,1,u	5960.13	5960.978	5958.747	2.231	0.054
1102011	2,3,1,u	5970.176	5971.024	5968.884	2.139	0.079
1012000	2,2,0,u	6080.673	6080.673	6080.1	0.573	-1.001
200111-1	2,2,0,u	6381.287	6381.287	6380.22	1.067	-0.033
RMS deviation					1.18	0.425

*) Empirical levels from work [**113**] in cm^{-1}. E" levels are empirical levels + B_0*J (B_0 = 0.8475 cm^{-1})

**) RMS deviation without two levels 2136.81(state $4\nu_5$) and 2660.198 (state $5\nu_5$).

Table 7. Vibrational levels of the $^{13}C_2H_2$ isotopologue up to 9700 cm^{-1}, in cm^{-1} units.

Vibr State		Empirical*	E"*	Calc	E"-Calc	E"-Calc++ 7 adjusted param
0001100	0, 1,1,g	603.888	605.008	603.5992	1.408	0.164
0000011	0, 1,1,u	728.352	729.472	729.5519	-0.080	-0.002
0002000	0, 2,0,g	1212.25	1212.250	1210.053	2.197	-0.171
000111-1	0, 2,0,u	1317.239	1317.239	1316.088	1.151	0.035
0001-111	0, 2,0,u	1329.611	1329.611	1328.124	1.487	0.334
0000020	0, 2,0,g	1445.29	1445.290	1445.592	-0.302	-0.118
0003100	0, 3,1,g	1828.406	1829.526	1826.466	3.059	-0.343
0100000	1, 3,0,g	1910.667	1910.667	1910.205	0.462	0.144
000221-1	0, 3,1,u	1921.337	1922.457	1920.21	2.247	0.040
0002011	0, 3,1,u	1940.924	1942.044	1939.759	2.284	0.094
0001120	0, 3,1,g	2036.403	2037.523	2036.714	0.809	-0.110
0001-122	0, 3,1,g	2054.138	2055.258	2053.869	1.388	0.416
0000031	0, 3,1,u	2164.654	2165.774	2166.166	-0.393	-0.046
0004000	0, 4,0,g	2448.74	2448.740	2445.486	3.254	-1.066
0101100	1, 4,1,g	2502.317	2503.437	2501.532	1.904	0.297
000311-1	0, 4,0,u	2531.614	2531.614	2530.99	0.624	-0.228
00022222	0, 4,0,g	2626.433	2626.433	2624.58	1.853	-0.102
0100011	1, 4,1,u	2637.218	2638.338	2637.904	0.434	0.180
0002-222	0, 4,0,g	2639.458	2639.458	2637.198	2.260	0.202
000113-1	0, 4,0,u	2743.421	2743.421	2742.991	0.430	-0.269
0000040	0, 4,0,g	2872.791	2872.791	2873.286	-0.495	0.041
0102000	1, 5,0,g	3098.25	3098.250	3096.727	1.523	-1.247
010111-1	1, 5,0,u	3213.395	3213.395	3211.776	1.619	0.131

0101-111	1, 5,0,u	3226.08	3226.080	3223.949	2.131	0.601
0010000	1, 5,0,u	3279.482	3279.482	3280.101	-0.619	-0.164
1000000	1, 5,0,g	3347.683	3347.683	3347.894	-0.211	-0.178
0100020	1, 5,0,g	3354.417	3354.417	3354.459	-0.042	-0.031
0200000	2, 6,0,g	3807.445	3807.445	3806.568	0.877	0.241
0102011	1, 6,1,u	3825.934	3827.054	3824.172	2.882	0.275
0011100	1, 6,1,u	3873.727	3874.847	3874.178	0.669	0.104
0101120	1, 6,1,g	3929.614	3930.734	3929.493	1.241	0.183
1001100	1, 6,1,g	3940.232	3941.352	3940.435	0.916	0.055
0010011	1, 6,1,g	4000.057	4001.177	4001.842	-0.665	-0.051
1000011	1, 6,1,u	4064.263	4065.383	4065.666	-0.283	-0.118
0100031	1, 6,1,u	4073.312	4074.432	4074.649	-0.217	0.019
010311-1	1, 7,0,u	4405.114	4405.114	4403.957	1.157	-0.144
0012000	1, 7,0,u	4472.357	4472.357	4470.897	1.460	-0.008
010222-2	1, 7,0,g	4507.807	4507.807	4505.471	2.336	-0.012
1002000	1, 7,0,g	4535.008	4535.008	4532.419	2.589	0.956
001111-1	1, 7,0,g	4581.506	4581.506	4580.991	0.515	0.016
0011-111	1, 7,0,g	4590.885	4590.885	4590.173	0.712	0.381
010113-1	1, 7,0,u	4632.526	4632.526	4631.729	0.797	-0.188
100111-1	1, 7,0,u	4645.566	4645.566	4644.985	0.581	-0.026
1001-111	1, 7,0,u	4653.976	4653.976	4652.819	1.157	0.352
0101-131	1, 7,0,u	4663.259	4663.259	4661.587	1.672	0.687
0010020	1, 7,0,u	4708.859	4708.859	4709.777	-0.918	-0.082
0100040	1, 7,0,g	4768.889	4768.889	4769.363	-0.474	-0.150
1000020	1, 7,0,g	4781.483	4781.483	4781.971	-0.488	0.005
0013100	1, 8,1,u	5078.635	5079.755	5077.456	2.299	0.012
020111-1	2, 8,0,u	5095.403	5095.403	5093.351	2.052	0.181
0110000	2, 8,0,u	5185.584	5185.584	5185.738	-0.154	-0.005
0200020	2, 8,0,g	5242.478	5242.478	5241.996	0.482	0.010
1002011	1, 8,1,u	5252.346	5253.466	5251.828	1.638	0.223
1100000	2, 8,0,g	5252.85	5252.850	5252.714	0.136	-0.011
0100051	1, 8,1,u	5476.377	5477.497	5478.03	-0.533	0.023
1000031	1, 8,1,u	5491.722	5492.842	5493.44	-0.599	0.189
0014000	1, 9,0,u	5688.088	5688.088	5686.496	1.592	-1.396
0111100	2, 9,1,u	5767.725	5768.845	5767.69	1.155	0.241
0020000	2,10,0,g	6490.556	6490.556	6491.427	-0.871	-0.168
020113-1	2,10,0,u	6509.974	6509.974	6508.736	1.238	-0.168
1010000	2,10,0,u	6521.919	6521.919	6522.301	-0.382	-0.197
110111-1	2,10,0,u	6535.122	6535.122	6534.582	0.540	0.016
0110020	2,10,0,u	6611.194	6611.194	6611.643	-0.449	0.094
2000000	2,10,0,g	6664.951	6664.951	6665.587	-0.636	-0.284
0210000	3,11,0,u	7077.504	7077.504	7077.295	0.209	0.050
0202-233	2,11,1,u	7097.612	7098.732	7096.188	2.543	0.405
1011100	2,11,1,u	7100.69	7101.810	7100.309	1.500	0.389
110221-1	2,11,1,u	7114.938	7116.058	7114.515	1.543	0.246
0111-122	2,11,1,u	7179.761	7180.881	7180.45	0.430	0.045
0111120	2,11,1,u	7197.123	7198.243	7197.127	1.116	0.758
0020011	2,11,1,u	7203.606	7204.726	7205.514	-0.789	0.116
1010011	2,11,1,g	7227.436	7228.556	7228.957	-0.402	-0.066
1101120	2,11,1,g	7244.462	7245.582	7244.931	0.651	0.345
2001100	2,11,1,g	7248.334	7249.454	7248.916	0.538	0.135
0200051	2,11,1,u	7361.65	7362.770	7362.832	-0.063	0.051
2000011	2,11,1,u	7372.263	7373.383	7374.177	-0.795	-0.131
1100031	2,11,1,u	7388.083	7389.203	7389.691	-0.488	0.160
0211100	3,12,1,u	7647.079	7648.199	7646.639	1.560	0.307
120111-1	3,13,0,u	8401.224	8401.224	8400.31	0.914	-0.250
1110000	3,13,0,u	8422.926	8422.926	8424.467	-1.541	-1.337
120311-1	3,15,0,u	9539.323	9539.323	9537.51	1.813	-0.769
1112000	3,15,0,u	9565.656	9565.656	9566.11	-0.454	-1.868
0030000	3,15,0,u	9605.325	9605.325			

021222-2	3,15,0,u	9612.150	9612.150	9609.431	2.719	0.963
012111-1	3,15,0,u	9662.073	9662.073	9663.76	-1.687	-1.742
RMS deviation**					1.33	0.43

*) Empirical levels from work [**113**] in cm^{-1}. E" levels are empirical levels + B_0*J (B_0 = 1.1195 cm^{-1})

**) RMS deviation without the level $3\nu_3$.

Conclusion

Comparisons with experimental data show that the ab initio PES of the electronic ground state of acetylene constructed in this work is currently the most accurate one. We note however, that the modeling of the PES shape versus the angular motion was more complicated than in the case of the recent ab initio study of another four-atomic molecule – formaldehyde [**78**]. This is because the harmonic term does not provide a dominant contribution to the frequency of the torsional motion, contrary to the case of formaldehyde. A quadratic approximation in the torsional variable does not work at all for the corresponding PES cut, which requires several higher-order terms for a satisfactory modeling. This particular shape could be thus more error sensitive in the calculation of rovibrational levels.

A full account of the Coriolis interactions using exact KEO together with the ab initio PES has permitted reliable predictions of splittings in (e-f) rovibrational doublets for Π, Δ, and Φ states. For the first time, the accuracy of ab initio values of the splittings is comparable to the experimental accuracy in high-resolution spectra. Note that the values of the splitting are quite robust with respect to an empirical optimization of the PES. This permitted testing the corresponding assignments in various bands. As a rule, the J-dependence of the splittings is smooth, but in some cases erratic outliers appear. This gives hints for possible errors in experimental assignments, which have to be checked during further analyses of the spectra. First-principles calculations thus provide an independent insight into uncertainties of available experimental data. A similar accuracy is obtained for vibrational levels of the isotopologues C_2D_2 (Table 9) and $^{13}C_2H_2$ (Table 10), confirming the reliability of the ab initio PES.

We have also produced an empirically optimized PES by adjusting 2 and 7 parameters to 120 experimental J = 0 and J=1 levels derived from high-resolution spectra with the RMS (obs.-calc.) deviation of 0.45 and 0.25 cm^{-1}. Band origins of C_2H_2 computed from these PES up to 7000 cm^{-1} are given in Table 4. Both the ab initio and the empirically optimized PES are provided in the Supplementary Materials as a C++ code.

For a further investigation of the corresponding accuracy issues, the ab initio PES can be used to derive effective spectroscopic models as it was done in the case of methane [**114**] [**115**]

[**116**]. This will permit to accurately compute physically meaningful values of the resonance coupling parameters from ab initio surface for advanced analyses of high-resolution spectra.

SUPPLEMENTARY MATERIAL

See supplementary material for the ab initio and the empirically optimized PES in orthogonal coordinates.

ACKNOWLEDGMENTS

The support of RNF-anr grant (Grant No. 22-42-09022) is acknowledged. Support from the French ANR TEMMEX project (Grant 21-CE30-0053-01) is acknowledged. The authors thank to Oleg Lyulin for a useful discussion. A.T. acknowledges support by the János Bolyai Research Scholarship of the Hungarian Academy of Sciences and by the ELTE New National Excellence Program (ÚNKP-21-5) financed by the Hungarian Ministry of Innovation and Technology and the Hungarian NKFIA Fund.

References

[1] G. Strey , I.M. Mills, *J. Mol. Spectrosc.*, 59, 103-115 **(1976)**.

[2] R. Wallace, *Chem. Phys.*, 88, 247-260 **(1984)**.

[3] R. Wallace, *Chem. Phys.*, 98, 197-205 **(1985)**.

[4] L. Halonen, M.S. Child, S. Carter, *Potential models and local mode vibrational eigenvalue calculations for acetylene.*, 47, 1097-1112 **(1982)**.

[5] W.D. Allen, Y. Yamaguchi, A.G. Császár, D.A. Clabo Jr., R.B. Remington, H.F. Schaefer III, *Chem. Phys.*, 145, 427-466 **(1990)**.

[6] M.J. Bramley, S Carter, N.C. Handy, I.M. Mills, *J. Mol. Spectrosc.*, 157, 301-336 **(1993)**.

[7] M.J. Bramley , N.C. Handy, *J. Chem. Phys.* , 98, 1378-1397 **(1993)**.

[8] D.W. Schwenke, *J. Chem. Phys.*, 100, 2867-2884 **(1993)**.

[9] J.M.L. Martin, T.J. Lee, P.R. Taylor, *J. Chem. Phys.*, 108, 676-691 **(1998)**.

[10] Z Zhang, B. Li, Z. Shen, Y. Ren, W. Bian, *Chem. Phys.*, 400, 1-7 **(2012)**.

[11] S. Joseph , A.J.C. Varandas, *J. Phys. Chem. A.* , 114, 13277-13287 **(2010)**.

[12] H. Lee, J.H. Baraban, R.W. Field, J.F. Stanton, *J. Phys. Chem. A.*, 117, 11679-11683 **(2013)**.

[13] D.A. Sadovskii , B.I. Zhilinskii, *Mol. Phys.*, 116, 3564-3601 **(2018)**.

[14] S. Carter , N.C. Handy, *Mol. Phys.*, 100, 681-698 **(2002)**.

[15] D. Xu, Li. G., D. Xie, H. Guo, *Chem. Phys. Lett.*, 365, 480-486 **(2002)**.

[16] D. Xu, H. Guo, S. Zou, J.M. Bowman, *Chem. Phys. Lett.*, 377, 582-588 **(2003)**.

[17] K.L. Chubb, A. Yachmenev, J. Tennyson, S.N. Yurchenko, *J. Chem. Phys.*, 149, 014101 **(2018)**.

[18] D. Jacquemart et al., *J. Quant. Spectrosc. Radiat. Transfer.*, 110, 717-732 **(2009)**.

[19] J. Vander Auwera, *J. Mol. Spectrosc.*, 201, 143-150 **(2000)**.

[20] H. Tran, J.-Y. Mandin, V. Dana, L. Régalia-Jarlot, X. Thomas, P. Von der Heyden, *J. Quant. Spectrosc. Radiat. Transfer.*, 108, 342-362 **(2007)**.

[21] O.M. Lyulin, D. Jacquemart, N. Lacome, V.I.,Mandin, J.-Y. Perevalov, *J. Quant. Spectrosc. Radiat. Transfer.*, 109, 1856-1874 **(2008)**.

[22] M. Herman, *Mol. Phys.*, 105, 2217-2241 **(2007)**.

[23] K.L. Chubb et al., *J. Quant. Spectrosc. Radiat. Transfer.* , 204, 42-55 **(2018)**.

[24] Robert. S, M. Herman, A Fayt, A. Campargue, S. Kassi, A. Liu, et al., *J. Quant. Spectrosc. Radiat. Transfer.*, 106, 2581–2605 **(2008)**.

[25] B Amyay, M. Herman, A Fayt, A. Campargue, S. Kassi, *J. Molec. Spectrosc.*, 267, 80-91 **(2011)**.

[26] O.M. Lyulin , A. Campargue, *J. Quant. Spectrosc. Radiat. Transfer.*, 203, 461–471 **(2017)**.

[27] O.M. Lyulin, A. Campargue, D Mondelain, S. Kassi, *J. Quant. Spectrosc. Radiat. Transfer.*, 130, 327-43 **(2013)**.

[28] O.M. Lyulin, D. Mondelain, S Béguier, S Kassi, J. Vander Auwera, A. Campargue, *J. Quant. Spectrosc. Radiat. Transfer.*, 108, 342-362 **(2007)**.

[29] O.M. Lyulin, J. Vander Auwera, A. Campargue, *J. Quant. Spectrosc. Radiat. Transfer.*, 160, 85-93 **(2015)**.

[30] M. Abbouti Temsamani, J.-M. Champion, S. Oss, *J. Chem. Phys.*, 110, 2893-2902 **(1999)**.

[31] A. Urru, I.N. Kozin, G. Mulas, B.J. Braams, J. Tennyson, *Mol. Phys.*, 108, 1973-1990 **(2010)**.

[32] J.K.G. Watson, *J. Molec. Spectrosc.*, 41, 229-230 **(1972)**.

[33] S.N. Yurchenko , T.M. Mellor, *J. Chem. Phys.*, 153, 154106 **(2020)**.

[34] P Jensen, *Can. J. Phys.*, 98, 506-511 **(2020)**.

[35] P. Jensen, M. Spanner, P.H. Bunker, *J. Molec. Structure*, 1212, 128087 **(2020)**.

[36] P.R. Bunker , P. Jensen, *Molecular Symmetry and Spectroscopy*, 2nd ed. Ottawa, Canada: NRC Research Press, 1998.

[37] K.L. Chubb, P. Jensen, S.N. Yurchenko, *Symmetry*, 137, 1-23 **(2018)**.

[38] F Klein, *Lectures on the icosahedron and the solution of equations of the fifth degree (Vorlesungen über das ikosaeder und die auflösung der gleichungen vom fünften grade)*. London, England: TRUBNER & CO., 1988.

[39] J.M. Brown et al., *J. Molec.Spectrosc.*, 55, 500-503 **(1975)**.

[40] T.M. Mellor, S.N. Yurchenko, P. Jensen, *Symmetry*, 13, 548 **(2021)**.

[41] V. Duflot et al., *Atmospheric Chemistry and Physics*, 15, 10509-10527 **(2015)**.

[42] C.A. Nixon, R.K. Achterberg, P.N. Romani, M. Allen, X. Zhang, N.A. Teanby, P.G. J. Irwin, F.M. Flasar, *Planetary and Space Science*, 58, 1667-1680 **(2010)**.

[43] H. Partridge , D.W. Schwenke, *J. Chem. Phys.*, 106, 4618-4639 **(1997)**.

[44] O.L. Polyansky, N.F. Zobov, S. Viti, J Tennyson, P.F. Bernath, L. Wallace, *Science*, 277, 346–8 **(1997)**.

[45] J. Tennyson, P. Barletta, M.A. Kostin, O.L. Polyansky, N.F. Zobov, *Spectrochimica Acta A*, 58, 663-672 **(2002)**.

[46] O. Polyansky, R. Ovsyannikov, A. Kyuberis, L. Lodi, J. Tennyson, N. Zobov, *J. Phys. Chem. A*, 117, 9633–9643 **(2013)**.

[47] X. Huang, D.W. Schwenke, S.A. Tashkun, et al., *J. Chem. Phys.*, 136, 124311 **(2012)**.

[48] X. Huang, R.S. Freedman, S.A. Tashkun, D.W. Schwenke, T.J. Lee, *J.Quant.Spectrosc.Radiat.Transf.*, 139, 134–46 **(2013)**.

[49] S.N. Yurchenko, R.J. Barber, A. Yachmenev, W. Thiel, P. Jensen, J. Tennyson, *J. Phys. Chem. A*, 113, 11845–11855 **(2009)**.

[50] T. Cours, P. Rosmus, V.G. Tyuterev, *J. Chem. Phys.*, 117, 5192–5208 **(2002)**.

[51] A.A. Azzam, L. Lodi, S.N. Yurchenko, J. Tennyson, *J.Quant.Spectrosc.Radiat.Transf.*, 161, 41-49 **(2015)**.

[52] X.C. Huang, D.W. Schwenke, Lee T.J., *J. Chem. Phys.*, 140, 114311 **(2014)**.

[53] Vl.G. Tyuterev, R.V. Kochanov, S.A. Tashkun, F. Holka, P.G. Szalay, *J. Chem. Phys.*, 139, 134307 **(2013)**.

[54] A. Barbe, S. Mikhailenko, E. Starikova, et al., *J. Quant. Spectrosc. Radiat. Transf.*, 130, 172-190 **(2013)**.

[55] Vl.G. Tyuterev, R.V. Kochanov, A. Campargue, S. Kassi, D. Mondelain, A. Barbe, *Phys.Rev.Lett*, 113, 143002 **(2014)**.

[56] V.G. Tyuterev, A. Barbe, D. Jacquemart, C. Janssen, S.N. Mikhailenko, E.N. Starikova, *J. Chem. Phys.*, 150, 184303 **(2019)**.

[57] R. Dawes, P. Lolur, J. Ma, H. Guo, *J. Chem. Phys.*, 135, 081102 **(2011)**.

[58] V. Kokoouline, D. Lapierre, A. Alijah, Vl.G. Tyuterev, *Phys. Chem. Chem. Phys.*, 22, 15885 - 15899 **(2020)**.

[59] C.H. Yuen, D. Lapierre, F. Gatti, V. Kokoouline, V.G. Tyuterev, *J. Chem. Phys.*, 123, 7733-7743 **(2019)**.

[60] M. Rey, A.V. Nikitin, V.G. Tyuterev, *Astrophys. J.*, 847, 105 **(2017)**.

[61] M. Rey, A.V. Nikitin, A. Campargue, S. Kassi, D. Mondelain, Vl.G. Tyuterev, *Phys. Chem.Chem. Phys.*, 16, 176-189 **(2016)**.

[62] A Wong, P.F. Bernath, M. Rey, A.V. Nikitin, V.G. Tyuterev, *Astrophys. J. Supplement Series*, 240, 4 **(2019)**.

[63] IvanovaY.A., Rey M., Tashkun S.A., Toon G.C., Sung, K., Tyuterev Vl.G. Nikitin A.V., *J. Quant. Spectrosc. Radiat. Transf.*, 203, 472-479 **(2017)**.

[64] M. Rey, I.S. Chizhmakova, A.V. Nikitin, Tyuterev Vl.G., *Phys. Chem.Chem. Phys.*, 20, 21008-21033 **(2018)**.

[65] X. Huang, D.W. Schwenke, T.J. Lee, *J. Chem. Phys.*, 134, 044320 **(2011)**.

[66] O. Egorov, M. Rey, A.V. Nikitin, D. Viglaska, *J. Phys. Chem. A.*, 125, 10568 **(2021)**.

[67] S.N. Yurchenko, M. Carvajal, W Thiel, P. Jensen, *J. Molec. Spectrosc.*, 239, 71-87 **(2006)**.

[68] C. Sousa-Silva, S.N. Yurchenko, J. Tennyson, *J. Molec. Spectrosc.*, 288, 28-36 **(2013)**.

[69] A.V. Nikitin, M. Rey, Vl.G Tyuterev, *J. Molec. Spectrosc*, 305, 40-47 **(2014)**.

[70] A. Owens, S.N. Yurchenko, A. Yachmenev, J. Tennyson, W. Thiel, *J. Chem. Phys.*, 142, 244306 **(2015)**.

[71] A. Owens, S.N. Yurchenko, A. Yachmenev, W. Thiel, *J. Chem. Phys.*, 143, 244317 **(2015)**.

[72] T. Delahaye, A. Nikitin, M. Rey, P. Szalay, Vl.G. Tyuterev, *J. Chem. Phys.*, 141, 104301 **(2014)**.

[73] T. Delahaye, A.V. Nikitin, M. Rey, P.G. Szalay, V.G. Tyuterev, *Chem. Phys. Letters*, 639, 275-282 **(2015)**.

[74] J. Li, S. Carter, J.M. Bowman, R. Dawes, D. Xie, H. Guo, *J. Phys. Chem. Lett.*, 5, 2364–2369 **(2014)**.

[75] A.V. Nikitin, M. Rey, I.S. Chizhmakova, Vl.G. Tyuterev, *J. Phys. Chem. A*, 124, 7014–7023 **(2020)**.

[76] A.V. Nikitin, M. Rey, Vl.G. Tyuterev, *J. Chem. Phys.*, 145, 114309 **(2016)**.

[77] W.J. Morgan et al., *J. Chem. Theory Comput.*, 14, 1333−1350 **(2018)**.

[78] A.V. Nikitin, A.E. Protasevich, A.A. Rodina, M. Rey, A. Tajti, V.G. Tyuterev, *Journal of Quantitative Spectroscopy & Radiative Transfer*, 260, 107478 **(2021)**.

[79] A. Yachmenev, S.N. Yurchenko, P. Jensen, W. Thiel, *J. Chem. Phys.*, 134, 244307-12 **(2011)**.

[80] O. Polyansky, A. Kyberis, N. Zobov, J. Tennyson, S. Yurchenko, L. Lodi, *MNRAS*, 480, 2597-2608 **(2018)**.

[81] X. Chapuisat , C. Iung, *Phys. Rev. A.*, 45, 6217-6235 **(1992)**.

[82] M. Mladenović, *J. Chem. Phys.*, 112, 1070-1081 **(2000)**.

[83] M Mladenovic, *J. Chem. Phys.*, 112, 1082-1095 **(2000)**.

[84] A.E. Protasevich , A.V. Nikitin, *Atmospheric and Oceanic Optics*, 35, 14-18 **(2022)**.

[85] A.V. Nikitin, F. Holka, Vl.G. Tyuterev, J. Fremont, *J. Chem. Phys*, 131, 244312 **(2009)**.

[86] A.V. Nikitin, M. Rey, Vl.G. Tyuterev, *Chem. Phys. Lett.*, 501, 179-186 **(2011)**.

[87] D.E. Woon , T.H. Dunning Jr., *J. Chem. Phys.*, 103, 4572 **(1995)**.

[88] H.-J. Werner, P.J. Knowles, G. Knizia, F.R. Manby, et al., *WIREs Comput Mol Sci*, 2, 242--253 **(2012)**.

[89] H.- J. Werner, P.J Knowles, R. Lindh, et. al.,.

[90] D.A. Varshalovich, A.N. Moskalev, V.K. Khersonskii, *Quantum theory of Angular momentum*.: World Scientific, 2008.

[91] M.J. Bramley, W.H. Jr. Green, Handy N.C., *Mol. Phys.*, 73, 1183–1208 **(1991)**.

[92] Born M. , K. Huang, *Dynamical theory of crystal lattices , Oxford at the Clarendon Press*. Oxford at the Clarendon Press: Clarendon Press, 1954.

[93] N.C. Handy, Y. Yamaguchi, H.F. Schaefer, *J. Chem. Phys.*, 84, 4481–4484 **(1986)**.

[94] W. Cencek , W. Kutzelnigg, *Chem. Phys. Lett.*, 266, 383 – 387 **(1997)**.

[95] J. Gauss, A. Tajti, M. Kállay, J.F. Stanton, P.G. Szalay, *J. Chem. Phys.*, 125, 144111 **(2006)**.

[96] A. Tajti, P.G. Szalay, J. Gauss, *J. Chem. Phys.*, 127, 014102 **(2007)**.

[97] P.G. Szalay, F. Holka, J. Fremont, M Rey, K.A. Peterson, Vl.G. Tyuterev, *Phys. Chem. Chem. Phys.*,

13, 3654–3659 **(2011)**.

[98] F. Holka, P.G. Szalay, J. Fremont, M. Rey, K.A. Peterson, Vl.G. Tyuterev, *J. Chem. Phys.*, 134, 094306 **(2011)**.

[99] J. Noga , R.J. Bartlett, *J. Chem. Phys.*, 86, 7041 **(1987)**.

[100] N. Oliphant , L. Adamowicz, *J. Chem. Phys.* , 95, 6645 **(1991)**.

[101] S.A. Kucharski , R.J. Bartlett, *J. Chem. Phys.*, 97, 4282 **(1992)**.

[102] Y.J. Bomble, J.F. Stanton, M. Kállay, J. Gauss, *J. Chem. Phys.*, 123, 054101 **(2005)**.

[103] D.A. Matthews , J.F. Stanton, *J. Chem. Phys.*, 142, 064108 **(2015)**.

[104] D.A. Matthews , J.F. Stanton, *J. Chem. Phys. 2015, 143, 204103*, 143, 204103 **(2015)**.

[105] A. Owens, S.N. Yurchenko, A. Yachmenev, J. Tennyson, W. Thiel, *J. Chem. Phys.*, 145, 104305 **(2016)**.

[106] J.F. Stanton, J. Gauss, M.E. Harding, P.G. Szalay, al. et. CFour program http://www.cfour.de.

[107] D.A. Matthews et al., *J. Chem. Phys.*, 152, 214108 **(2020)**.

[108] R. Perez, J.M. Brown, Y. Utkin, J. Han, R.F. Curl, *J. Molec. Spectrosc.*, 236, 151-157 **(2006)**.

[109] A. Perrin, A. Valentin, L. Daumont, *J. molec. struct.*, 780–781, 28-44 **(2006)**.

[110] J. Flaud, W. Lafferty, R. Sams, S. Sharpe, *Molec. Phys.*, 104, 1891 **(2006)**.

[111] R.J. Bouwens, J.A. Hammerschmidt, M.M. Grzeskowiak, T.A. Stegink, P.M. Yorba, W.F. Polik, *J. Chem. Phys.*, 104, 460 **(1996)**.

[112] M. Kállay et al., *J. Chem. Phys.*, 152, 074107 **(2020)**.

[113] M. Herman, A. Campargue, M.I. El Idrissi, J. Vander Auwera, *J. Phys. Chem. Ref. Data*, 32, 921 **(2003)**.

[114] Vl.G. Tyuterev, S.A. Tashkun, M. Rey, R.V. Kochanov, A.V. Nikitin, T. Delahaye, *J.Phys.Chem. A*, 117, 13779-13805 **(2013)**.

[115] A.V. Nikitin et al., *J. Quant. Spectrosc. Radiat. Transfer*, 219, 323–332 **(2018)**.

[116] A.V. Nikitin, A.E. Protasevich, M. Rey, V.G. Tyuterev, *J. Chem. Phys.*, 149, 124305 **(2018)**.

[117] D.C. Burleigh , E.L. Sibert, *J. Chem. Phys.*, 98, 8419-8431 **(1993)**.

[118] D.C. Burleigh, A.B. McCoy, E.L. III Sibert, *J. Chem. Phys*, 104, 480 **(1996)**.

[119] T.J. Lukka, *J. Chem. Phys.*, 102, 3945 **(1995)**.

[120] S.M. Colwell , N.C. Handy, *Molec. Phys.*, 92, 317 **(1997)**.

[121] M.J. Bramley , T.Jr. Carrington, *J. Chem. Phys.*, 99, 8519-8541 **(1993)**.

[122] S. Brünken, H.S. P. Müller, F. Lewen, *Phys. Chem. Chem. Phys.*, 5, 1515−1518 **(2003)**.

[123] H.S.P. Muller, G. Winnewisser, J. Demaison, A. Perrin, A. Valentin, *J. Molec. Spectrosc.*, 200, 143-144 **(2000)**.

[124] H.S.P. Muller , F. Lewen, *J. Molec. Spectrosc.*, 331, 28-33 **(2017)**.

[125] A. Perrin, F. Keller, J.-M. Flaud, *J. Molec. Spectrosc.*, 221, 192-198 **(2003)**.

[126] A. Perrin, J.-M. Flaud, A. Predoi-Cross, M. Winnewisser, B.P. Winnewisser, G. Mellau, M. Lock, *J. Molec. Spectrosc.*, 187, 61-69 **(1998)**.

[127] M. Rey, *J. Chem. Phys.*, 151, 024101 **(2019)**.

[128] M. Rey, A.V. Nikitin, V.G. Tyuterev, *J. Chem. Phys*, 136, 244106 **(2012)**.

[129] J. Lohilahti , S. Alanko, *J. Molec. Spectrosc.*, 205, 248-251 **(2001)**.

[130] J. Lohilahti, O.N. Ulenikov, E.S. Bekhtereva, S. Alanko, R. Anttila, *J.Molec. Structure*, 780-781, 182-205 **(2006)**.

[131] G.C. Rhoderick , W.D. Dorko, *Environ. Sci. Technol.*, 38, 2685-2692 **(2004)**.

[132] D.T. Allen, V.M. Torres, J. Thomas, e et al, *PNAS*, 110, 17768–17773 **(2013)**.

[133] D.R. Caultona, P.B. Shepsona, R.L. Santoro, et al, *PNAS*, 111, 6237–6242 **(2014)**.

[134] K. McKain, A. Down, S.M. Raciti, e et al, *PNAS*, 112, 1941–1946 **(2015)**.

[135] M.A.K. Khalil, M.J. Shearer, R.A. Rasmussen, *Methane Sinks Distribution in Atmospheric Methane: Sources, Sinks, and Role in Global Change*, M.A.K. Khalil, Ed. Berlin, Heidelberg: Springer, 1993.

[136] G. Tinetti, T. Encrenaz, A. Coustenis, *Astron Astrophys Rev*, 21, 63 **(2013)**.

[137] M. Hirtzig et al., *Icarus*, 226, 470-486 **(2013)**.

[138] B. Bezard, *Icarus*, 242, 64-73 **(2014)**.

[139] P.F. Bernath, *Phil. Trans. R Soc. A*, 372, 20130087 **(2014)**.

[140] J. Tennyson , S.N. Yurchenko, *Molecular Astrophysics*, 8, 1-18 **(2017)**.

[141] M.R. Swain, P. Deroo, C.A. Griffith, G. Tinetti, et al., *Nature*, 463, 637 **(2010)**.

[142] J.I. Moses, C. Visscher, J.J. Fortney, et al., *ApJ*, 737, 15 **(2011)**.

[143] R. Hu , S. Seager, *ApJ*, 784, 63 **(2014)**.

[144] B. Macintosh, J.R. Graham, T. Barman, *Science*, 350, 64-67 **(2015)**.

[145] B.R. Oppenheimer, S.R. Kulkarni, K. Matthews, T. Nakajima, *Science*, 270, 1478 **(1995)**.

[146] S.K. Legget, M.S. Marley, R. Freedmann, et al., *ApJ*, 667, 537 **(2007)**.

[147] T. Nakajima, T. Tsuji, K. Yanagissawa, *ApJ*, L119, 561 **(2001)**.

[148] M.C. Cushing, J.D. Kirkpatrick, C.R. Gelino, et al., *ApJ*, 743, 50 **(2011)**.

[149] H. Partridge , D.W. Schwenke, *J. Chem. Phys.*, 106, 4618-4639 **(1997)**.

[150] O.L. Polyansky, N.F. Zobov, S. Viti, J Tennyson, P.F. Bernath, L. Wallace, *Science*, 277, 346–8 **(1997)**.

[151] O. Polyansky, R. Ovsyannikov, A. Kyuberis, L. Lodi, J. Tennyson, N. Zobov, *J. Phys. Chem. A 117*, 117, 9633–9643 **(2013)**.

[152] O. Polyansky, K. Bielska, M. Ghysels, L. Lodi, N. Zobov, J. Hodges, J. Tennyson, *Phys. Rev. Lett.*, 114, 243001 **(2015)**.

[153] SchwenkeD.W. , Lee T.J. Huang X.C., *J. Chem. Phys.*, 140, 114311 **(2014)**.

[154] D. Lapierre, A. Alijah, R. Kochanov, V. Kokoouline, Vl. Tyuterev, *Phys. Rev. A*, A94, 042514 **(2016)**.

[155] J.-P. Champion, M. Loete, G. Pierre, *Spectroscopy of the Earth's Atmosphere and Interstellar Medium in: K.N. Rao, A.Weber (Eds.)*. San Diego: Academic Press, 1992.

[156] B.I. Zhilinskii, V.I. Perevalov, Vl.G. Tyuterev, *Method of Irreducible Tensorial Operators in the Theory of Molecular Spectra*. Novosibirsk: Nauka [in russian], 1987.

[157] M. Rey, A.V. Nikitin, Vl.G. Tyuterev, *The Astrophysical Journal*, 789, 2 **(2014)**.

[158] S.N. Yurchenko , J. Tennyson, *Monthly Notices of the Royal Astronomical Society*, 440, 1649-1661 **(2014)**.

[159] S.N. Yurchenko, D.S. Amundsen, J. Tennyson, I.P. Waldmann, *Astronomy and Astrophysics*, 605, A95 **(2017)**.

[160] M Rey, A.V. Nikitin, B. Bézard, P. Rannou, A. Coustenis, V.G. Tyuterev, *Icarus*, 303, 114-130 **(2018)**.

[161] J. Thievin, R. Georges, S. Carles, B. Abdessamad, B. Rowe, J.P. Champion, *J. Quant. Spectrosc. Radiat. Transfer.*, 109, 2027 **(2008)**.

[162] R.J. Hargreaves, C.A. Beale, L. Michaux, M. Irfan, P.F. Bernath, *The astrophysical journal*, 757, 46 **(2012)**.

[163] B.P. F. Hargreaves, J. Bailey, M. Dulick, *ApJ*, 813, 1 **(2015)**.

[164] B. Amyay, A. Gardez, R. Georges, L. Biennier, J. Vander Auwera, C. Richard, V. Boudon, *J. Chem. Phys.*, 148, 134306 **(2018)**.

[165] S.N. Yurchenko, J. Tennyson, J. Bailey, M.D. J. Hollis, G. Tinetti, *PNAS*, 111, 9379–9383 **(2014)**.

[166] J. Tennyson , S.N. et al. Yurchenko, *J. Molec. Spectrosc.*, 327, 73–94 **(2016)**.

[167] M. Rey, A.V. Nikitin, Y. Babikov, Vl.G. Tyuterev, *J. Molec. Spectrosc.*, 327, 138–158 **(2016)**.

[168] C. Wenger , J.-P. Champion, *J. Quant. Spectrosc. Radiat. Transfer*, 59, 471 **(1998)**.

[169] Vl.G. Tyuterev, S.A. Tashkun, M. Rey, R.V. Kochanov, A.V. Nikitin, T. Delahaye, *J. Phys. Chem.*, 117, 13779−13805 **(2013)**.

[170] S. Albert, S. Bauerecker, V. Boudon, L.R. Brown, J.-P. Champion, M. Loete, A.V. Nikitin, M. Quack, *Chem Phys*, 358, 131-146 **(2009)**.

[171] A.V. Nikitin, V. Boudon, Ch. Wenger, S. Albert, L.R. Brown, S. Bauerecker, M. Quack, *PCCP*, 15, 10071-10093 **(2013)**.

[172] L. Daumont et al., *J. Quant. Spectrosc. Radiat. Transfer*, 116, 101-109 **(2013)**.

[173] M. Rey, A.V. Nikitin, Vl.G. Tyuterev, *J. Quant. Spectrosc. Radiat. Transfer.*, 164, 207–220 **(2015)**.

[174] Y.A. Ba et al., *J. Quant. Spectrosc. Radiat. Transfer.*, 130, 62-68 **(2013)**.

[175] B. Amyay, M. Louviot, O. Pirali, R. Georges, J. Vander Auwera, V. Boudon, *J. Chem. Phys.*, 144, 024312 **(2016)**.

[176] B. Amyay, A. Gardez, R. Georges, L. Biennier, J. Vander Auwera, C. Richard, V. Boudon, *J. Chem. Phys.*, 148, 169902 **(2018)**.

[177] A.V. Nikitin, X. Thomas, L. Regalia, L. Daumont, P. Von der Heyden, Vl.G. Tyuterev, *J. Quant. Spectrosc. Radiat. Transfer*, 112, 28-40 **(2011)**.

[178] A.V. Nikitin, M. Rey, S.A. Tashkun, S. Kassi, D. Mondelain, A. Campargue, Vl.G. Tyuterev, *J. Quant. Spectrosc. Radiat. Transfer*, 168, 207–216 **(2016)**.

[179] X.-G. Wang , T. Carrington Jr., *The Journal of Chemical Physics*, 121, 2937-2954 **(2004)**.

[180] X.G. Wang , T. Carringhton, *The Journal of Chemical Physics*, 118, 6260 **(2003)**.

[181] X.-G. Wang , T. Carrington Jr., *The Journal of Chemical Physics*, 138, 104106 **(2013)**.

[182] H.-G. Yu, *Journal of Chemical Physics*, 117, 2030-2037 **(2002)**.

[183] P. Cassam-Chenai, Y. Bouret, M. Rey, S.A. Tashkun, NikitinA. V., Vl.G. Tyuterev, *Int J. Quant. Chem.*,

112, 2201–2220 **(2012)**.

[184] S. Carter, A.R. Sharma, J.M. Bowman, *Journal of Chemical Physics*, 137, 154301 **(2012)**.

[185] H.-G. Yu, *Journal of Chemical Physics*, 121, 6334-6340 **(2004)**.

[186] Z. Zhao, J. Chen, Z. Zhang, D.H. Zhang, X.-G. Wang, T.Jr. Carrington, F. Gatti, *J. Chem. Phys.*, 148, 074113 **(2018)**.

[187] S.N. Yurchenko, W. Thiel, P. Jensen, *J. Mol. Spectrosc.*, 245, 126-140 **(2007)**.

[188] E Matyus, J Simunek, A Csaszar, *J. Chem. Phys.*, 131, 074106 **(2009)**.

[189] S.N. Yurchenko, A. Yachmenev, R.I. Ovsyannikov, *J. Chem. Theory and Comp.*, 4368-4381 **(2017)**.

[190] A. Yachmenev , S.N. Yurchenko, *J. Chem. Phys.*, 143, 014105 **(2015)**.

[191] L.R. Brown, *JQSRT*, 96, 251-270 **(2005)**.

[192] S. Béguier, A.W. Liu, A. Campargue, *JQSRT*, 166, 6-12 **(2015)**.

[193] D.N. Kozlov, D.A. Sadovskii, P.P. Radi, *J Mol. Spectriosc.*, 291, 23-32 **(2013)**.

[194] Neil Bowles, R. Passmore, K. Smith, G. Williams, S. Calcutt, P.G.J. Irwin, *J. Quant. Spectrosc. Radiat. Transfer*, 113, 763–782 **(2012)**.

[195] T.J. Lee, J.M.L. Martin, P.R. Taylor, *J. Chem. Phys.*, 102, 254-261 **(1995)**.

[196] R. Marquardt , M. Quack, *J. Phys. Chem.*, 108, 3166-3181 **(2004)**.

[197] D.W. Schwenke , H. Partridge, *Spectrochim. Acta A*, 57, 887-895 **(2001)**.

[198] C. Oyanagi, K. Yagi, T. Taketsugu, K. Hirao, *J. Chem.Phys.*, 124, 064311 **(2006)**.

[199] M Majumder, S.E. Hegger, R. Dawes, S. Manzhos, X.-G. Wang, T.Jr. Carrington, Lid J., H. Guo, *Molecular Physics*, 113, 1823-1833 **(2015)**.

[200] X.-G. Wang , T.,Jr. Carrington, *The Journal of Chemical Physics*, 141, 154106 **(2014)**.

[201] L. Halonen , M.S. Child, *Molec. Phys.*, 46, 239-255 **(1982)**.

[202] O.N. Ulenikov, E.S. Bekhtereva, S. Albert, S. Bauerecker, H.M. Niederer, M. Quack, *J. Chem. Phys.*, 141, 234302 **(2014)**.

[203] J.K.G. Watson, *Molecular Physics*, 15, 479 **(1968)**.

[204] A.V. Nikitin, M. Rey, Vl.G. Tyuterev, *J. Chem. Phys.*, 142, 094118 **(2015)**.

[205] William Hart. http://www.mpir.org/.

[206] A.E. Protasevich , A.V. Nikitin, *Molec. Phys.*, 116, 44-53 **(2018)**.

[207] A Campargue, O Leshchishina, L Wang, D Mondelain, Kassi S., *J. Molec. Spectrosc.*, 291, 16-22 **(2013)**.

[208] S Béguier, S Kassi, A. Campargue, *J. Molec. Spectrosc.*, 208, 1-5 **(2015)**.

[209] G. Pierre, J.-C. Hilico, C. de Bergh, J.-P. Maillard, *J. Mol. Spectrosc.*, 82, 379–393 **(1980)**.

[210] A. De Martino, R. Frey, F. Pradère, *Molecular Physics*, 55, 731-749 **(1985)**.

[211] A. De Martino, R. Frey, F. Pradere, *Chem. Phys. Lett.*, 111, 113-116 **(1984)**.

[212] M. Chevalier , A. De Martino, *Chem. Phys. Lett.*, 135, 446-450 **(1987)**.

[213] A. Campargue , D.,Jost, R. Permogorov, *J. Chem. Phys.*, 102, 5910-5916 **(1995)**.

[214] K. Boraas, Z. Lin, J.P. Reilly, *J. Chem. Phys.*, 100, 7916-7927 **(1994100)**.

[215] G. HERZBERG, *Infrared and Raman Spectra*. New York, USA: Van Nostrand Comp., 1945.

[216] A.V. Nikitin, M. Rey, Vl.G. Tyuterev, *J. Quant. Spectrosc. Radiat. Transfer*, 200, 90-99 **(2017)**.

[217] A. Campargue, O. Leshchishina, D. Mondelain, S. Kassi, A. Coustenis, *J. Quant. Spectrosc. Radiat. Transfer*, 118, 49-59 **(2013)**.

[218] A.V. Nikitin, M. Rey, V.G. Tyuterev, *Chem. Phys.Lett.*, 565, 5-11 **(2013)**.

[219] E. Karkoschka , M.G. Tomasko, *Icarus*, 205, 674–694 **(2010)**.

[220] J.P. Champion, J-C Hilico, L.R. Brown, *J. Mol. Spectrosc.*, 208, 244-255 **(1989)**.

[221] AlexanderE. Protasevich, Alena A. Rodina, Michael Rey, Attila Tajti, and Vladimir G. Tyuterev Andrei V. Nikitin. (2020) A New high precision potential energy surface and vibrational levels of formaldehyde. supplemental material.

[222] Al-Refaie A. F., Yachmenev A., Tennyson J., Yurchenko S. N., "ExoMol line lists – VIII. A variationally computed line list for hot formaldehyde," *MNRAS*, vol. 448, pp. 1704-1714, 2015.

[223] M. Mladenovic, *Spectrochimica Acta Part A*, 58, 809-824 **(2002)**.

[224] J. Makarewicz , A. Skalozub, *J. Phys. Chem. A.*, 111, 7860-7869 **(2007)**.

[225] M. Rey, A.V. Nikitin, Vl.G. Tyuterev, *Phys. Chem.Chem. Phys.*, 15, 10049-10061 **(2013)**.

[226] K. Yagi, C. Oyanagi, T. Taketsugu, K. Hirao, *J. Chem. Phys.*, 118, 1653-1660 **(2003)**.

[227] H.S. P. Müller , F. Lewen, *J. Molec. Spectrosc.*, 331, 28−33 **(2017)**.

[228] A. Barbe, P. Marche´, C. Secroun, P. Jouve, *J. Geophys. Res. Lett.*, 6, 463–465 **(1979)**.

[229] P. Khare, N. Kumar, K.M. Kumari, S.S. Srivastave, *Rev. Geophys.*, 37, 227 **(1999)**.

[230] P. Kakabokas, P. Carlier, P. Fresnet, G. Mouvierg, G. Toupance, *Atmos. Environ.*, 22, 147-155 **(1988)**.

[231] N.M. Poulin, M.J. Bramley, CarringtonT. Jr., H.G. Kjaergaard, B.R. Henry, *J. Chem. Phys.*, 104, 7807-7820 **(1996)**.

[232] L. Zhu et al., *Atmos. Chem. Phys.*, 20, 12329–12345 **(2020)**.

[233] T. Steck, N. Glatthor, T. Von Clarmann, H. Fischer, J.M. Flaud, B. Funke, U. Grabowski, M. Höpfner, *Atmos. Chem. Phys.*, 8, 463-470 **(2008)**.

[234] G. Dufour, S. Szopa, M.P. Barkley, C.D. Boone, A. Perrin, P.I. Palmer, P.F. Bernath, *Atmos. Chem. Phys.*, 9, 3893-3910 **(2009)**.

[235] S. Joseph , A.J.C. Varandas, *J. Phys. Chem. A.* , 114, 13277-13287 **(2010)**.

[236] J.M. L. Martin , T.J. Lee, *J. Molec. Spectrosc.*, 160, 105-116 **(1993)**.

693

694